2022

Simulated Response of St. Joseph Bay, Florida, Seagrass Meadows and Their Belowground Carbon to Anthropogenic and Climate Impacts

Marie Cindy Lebrasse

Blake A. Schaeffer

Richard C. Zimmerman
Old Dominion University, rzimmerm@odu.edu

Victoria J. Hill
Old Dominion University, vhill@odu.edu

Megan M. Coffer

See next page for additional authors

Original Publication Citation

Lebrasse, M. C., Schaeffer, B. A., Zimmerman, R. C., Hill, V. J., Coffer, M. M., Whitman, P. J., Salls, W. B., Graybill, D. D., & Osburn, C. L. (2022). Simulated response of St. Joseph Bay, Florida, seagrass meadows and their belowground carbon to anthropogenic and climate impacts. *Marine Environmental Research*, *179*, 1-16, Article 105694. https://doi.org/10.1016/j.marenvres.2022.105694

Marine Environmental Research 179 (2022) 105694

Contents lists available at ScienceDirect

Marine Environmental Research

journal homepage: www.elsevier.com/locate/marenvrev

Simulated response of St. Joseph Bay, Florida, seagrass meadows and their belowground carbon to anthropogenic and climate impacts

Marie Cindy Lebrasse [a,b,*], Blake A. Schaeffer [c], Richard C. Zimmerman [d], Victoria J. Hill [d], Megan M. Coffer [a], Peter J. Whitman [a], Wilson B. Salls [c], David D. Graybill [a], Christopher L. Osburn [b]

[a] Oak Ridge Institute for Science and Education, U.S. Environmental Protection Agency, Durham, NC, USA
[b] Department of Marine, Earth and Atmospheric Sciences, North Carolina State University, Raleigh, NC, USA
[c] U.S. Environmental Protection Agency, Office of Research and Development, Durham, NC, USA
[d] Department of Ocean and Earth Sciences, Old Dominion University, Norfolk, VA, USA

ARTICLE INFO

Keywords:
Seagrass
Climate
Water quality
GrassLight
Submerged aquatic vegetation

ABSTRACT

Seagrass meadows are degraded globally and continue to decline in areal extent due to human pressures and climate change. This study used the bio-optical model *GrassLight* to explore the impact of climate change and anthropogenic stressors on seagrass extent, leaf area index (LAI) and belowground organic carbon (BGC) in St. Joseph Bay, Florida, using water quality data and remotely-sensed sea surface temperature (SST) from 2002 to 2020. Model predictions were compared with satellite-derived measurements of seagrass extent and shoot density from the Landsat images for the same period. The *GrassLight*-derived area of potential seagrass habitat ranged from 36.2 km^2 to 39.2 km^2, averaging 38.0 ± 0.8 km^2 compared to an observed seagrass extent of 23.0 ± 3.0 km^2 derived from Landsat (range = 17.9–27.4 km^2). *GrassLight* predicted a mean seagrass LAI of 2.7 m^2 leaf m^{-2} seabed, compared to a mean LAI of 1.9 m^2 m^{-2} estimated from Landsat, indicating that seagrass density in St. Joseph Bay may have been below its light-limited ecological potential. Climate and anthropogenic change simulations using *GrassLight* predicted the impact of changes in temperature, pH, chlorophyll *a*, chromophoric dissolved organic matter and turbidity on seagrass meadows. Simulations predicted a 2–8% decline in seagrass extent with rising temperatures that was offset by a 3–11% expansion in seagrass extent in response to ocean acidification when compared to present conditions. Simulations of water quality impacts showed that a doubling of turbidity would reduce seagrass extent by 18% and total leaf area by 21%. Combining climate and water quality scenarios showed that ocean acidification may increase seagrass productivity to offset the negative effects of both thermal stress and declining water quality on the seagrasses growing in St. Joseph Bay. This research highlights the importance of considering multiple limiting factors in understanding the effects of environmental change on seagrass ecosystems.

1. Introduction

Seagrasses (submerged flowering plants) form extensive meadows in shallow coastal waters worldwide, providing important ecosystem services such as shoreline stabilization, maintenance of water quality and provision of food and habitat to many marine organisms (Barbier et al., 2011; Lefcheck et al., 2019). Despite growing recognition of the global importance of these coastal ecosystems, particularly as a major carbon sink (Prentice et al., 2019; Berger et al., 2020), seagrasses are in global decline due to stressors such as increased sediment loading, coastal eutrophication, mechanical disturbance, and climate change (Orth et al., 2006; Waycott et al., 2009; Unsworth et al., 2019). With 40% of the world's human population living in coastal areas, the magnitude of human pressure on seagrasses is increasing. Coastal development and nutrient enrichment have historically been responsible for global seagrass declines (Fraser and Kendrick, 2017), as shown by a 29% global loss in seagrass coverage since the 1980s (Waycott et al., 2009; Short et al., 2011), and seagrasses continue to be lost at a rate of 1.4% per year (Short et al., 2011). In Florida, eutrophication was linked to an increase in anthropogenic disturbances to seagrass meadows (Tomasko et al.,

* Corresponding author. Oak Ridge Institute for Science and Education, U.S. Environmental Protection Agency, Durham, NC, USA.
E-mail address: cmlebras@ncsu.edu (M.C. Lebrasse).

https://doi.org/10.1016/j.marenvres.2022.105694
Received 14 February 2022; Received in revised form 22 June 2022; Accepted 23 June 2022
Available online 30 June 2022

2005) and seagrasses there remain vulnerable to nuisance algal blooms that reduce light availability (Han et al., 2016; Hughes et al., 2018; Rasmusson et al., 2020). The global implications of these habitat losses are dire but sustained local and regional efforts to improve water transparency by reducing nutrient loading has led to seagrass recovery in Chesapeake Bay, USA (Lefcheck et al., 2018), Tampa and Sarasota Bays, USA (Greening et al. 2011, 2018; Sherwood et al., 2017; Tomasko et al., 2018), and some European estuaries (de Los Santos et al., 2019).

Physical factors such as substratum, wave scour, and biological interactions such as grazing by herbivores influence the growth and distribution of seagrass. However, the main factor affecting seagrass is the quality and clarity of coastal waters (Unsworth et al. 2018, 2019; Griffiths et al., 2020). This reflects the fact that seagrasses have some of the highest light requirements of any marine autotroph (Dennison et al., 1993; Zimmerman, 2021), especially in Florida where they have been found to require up to 58% of surface irradiance (Choice et al., 2014; Beck et al., 2018). The quantity and quality of light available to seagrass is affected by anthropogenic activities through increasing concentrations of suspended sediments, chlorophyll *a* (Chl *a*), and chromophoric dissolved organic matter (CDOM; Orth et al., 2006), all of which attenuate light and reduce the depth range of seagrass habitat (Duarte 1991). Light attenuation due to increased water turbidity often results from dredging activities (McMahon et al., 2011), flood plumes (Collier et al., 2012; Petus et al., 2014), and sediment resuspension that may be exacerbated following seagrass loss (van der Heide et al., 2007, Rodemann et al., 2021). Increased coastal development and catchment modification often result in nutrient enrichment (Lapointe et al., 2020) that increase phytoplankton populations leading to nuisance algal blooms (Webster and Harris, 2004), and promote epiphyte growth on seagrass leaves (Lee et al., 2007) further limiting light availability. Both turbidity events (Longstaff and Dennison, 1999; Davis et al., 2016) and increased phytoplankton abundances (Johansson, 2002; Brand and Compton, 2007) were found to cause extensive seagrass loss.

Impacts of local water quality deterioration can be exacerbated by climate change, which represents a global threat to seagrass populations. For instance, increases in precipitation and changes in the frequency of storms and heavy rainfall events can result in large pulses of terrestrial sediment, organic matter and dissolved nutrients into coastal systems (Nunes et al., 2009; Capuzzo et al., 2015) that further reduces light availability, a process that has been called coastal darkening (Aksnes et al., 2009). The implications of coastal darkening under climate-driven environmental changes have been demonstrated for primary producers (Mustaffa et al., 2020) and kelp forests (Blain et al., 2021) but its effects on seagrass ecosystems have not been shown. Hence long-term decline in water quality conditions and decreased light availability continue to cause localized impacts on seagrass meadows (Wooldridge, 2017), and are often compounded by the stress associated with global climate change (Zimmerman et al., 2015; Hall et al., 2016; Unsworth et al., 2019).

Ocean warming is a significant challenge for seagrass ecosystems globally, especially when combined with poor water quality (Moore et al., 2012; Hall et al., 2016; Carlson et al., 2018; Rodemann et al., 2021). Marine heatwaves, in particular, have caused extensive diebacks of diverse seagrass meadows in Shark Bay, Australia (Strydom et al., 2020), and periodic die-backs of *Zostera marina* and *Ruppia maritima* in the Chesapeake Bay (Moore et al., 2012; Richardson et al., 2018), and *Thalassia testudinum* (turtlegrass) in Florida Bay (Hall et al., 2016; Carlson et al., 2018). While temperature has been shown to affect seagrass abundance and productivity (Zimmerman et al., 2015), studies indicate that both temperate and tropical seagrasses are likely to benefit from ocean acidification (reviewed in Zimmerman, 2021). Ocean acidification increases the concentration of dissolved aqueous carbon dioxide (CO_2), which is a critical and often limiting substrate for seagrass photosynthesis (Beer et al., 2002; Zimmerman et al., 2017). As such, increased availability of CO_2 in surface waters via ocean acidification may prove beneficial to seagrasses given CO_2-limitation as shown in previous studies (Zimmerman et al. 1997, 2017; Jiang et al., 2010; Campbell and Fourqurean, 2013; Egea et al., 2018; Pacella et al., 2018). The Intergovernmental Panel on Climate Change Fifth Assessment Report (IPCC, 2014) presented four Representative Concentration Pathways (RCPs) to project how greenhouse gas (GHG) emissions and subsequent radiative forcing will impact the global climate by 2100. Across the four RCPs, temperature is predicted to increase between 1.0 and 3.7 °C and ocean pH is predicted to drop between 0.07 and 0.31 units. It has been shown that organisms are more sensitive to a given stressor when simultaneously affected by another (Paine et al., 1998), and seagrasses are often subjected to multiple co-stressors, such as heat waves and poor water quality, at the same time. Predicting the response of seagrasses to the combined effects of global climate change and watershed-scale deterioration in water quality will be critical to determine the persistence of seagrass in coastal environments throughout the world.

The relatively clear waters of St. Joseph Bay Florida along with their low-energy environment permit a high diversity of aquatic plants and animals to thrive (Valentine and Heck, 1993; Beck and Odaya, 2001), which serves as an ideal natural laboratory to study the stability of its seagrass beds in an otherwise dynamic seascape where coastal development has disturbed many other areas (e.g., Florida Bay, Tampa Bay and Chesapeake Bay). This study seeks to compare predictions of the light-limited distribution and density of seagrass in St. Joseph Bay derived from the bio-optical model *GrassLight* (Zimmerman, 2003a, 2006; Zimmerman et al., 2015) with remotely-sensed observations derived from the Landsat satellite series presented in Lebrasse et al. (2022) over an 18-year period from 2002 to 2020 that showed long-term stability in seagrass extent. Comparing the *GrassLight* estimates of the light-limited seagrass extent, leaf area index (LAI) and belowground organic carbon (BGC) to Landsat-derived estimates will help assess potential drivers of seagrass coverage and carbon storage in the bay. Results from 2020 were used in combination with climate projections and projected water quality changes to estimate the influence of potential future scenarios on the tropical seagrass ecosystem of St. Joseph Bay. Altogether, this study aims to address the extent to which the distribution and density of the seagrass population of St. Joseph Bay is controlled by light availability and to explore the combined impacts of local water quality and global climate change on this population through the 21st Century.

2. Methods

A time series of Landsat imagery was previously analyzed to estimate seagrass extent, LAI and BGC (section 2.2) in St. Joseph Bay, Florida (Lebrasse et al., 2022). We summarize the method briefly here and in the flowchart in Fig. 1. *GrassLight* is a bio-optical model that predicts optimal values of LAI and biomass based on water column optical conditions and submerged plant canopy architecture (Zimmerman, 2003). Water quality data extracted from the University of South Florida Virtual Buoy System (VBS; https://optics.marine.usf.edu/; Hu et al., 2013) were used for *GrassLight* simulations of light-limited seagrass extent, LAI and BGC (for each year) between 2002 and 2020 (sections 2.3-2.5). Landsat observations were compared to *GrassLight* predictions using a Wilcoxon-signed rank test (section 2.6). The final step leveraged changes in temperature and pH forecast under four RCPs (IPCC, 2014) as well as hypothetical changes in water quality to determine the response of seagrass communities in St. Joseph Bay to the combined impacts of these potential stressors (section 2.7).

2.1. Study site

St. Joseph Bay, a shallow, subtropical lagoon covering ~200 km^2 on the northwestern Florida panhandle (29.8° N, 85.5° W), is one of the most pristine coastal bays in Florida. It is bounded on the west by the St. Joseph Peninsula, on the east by the Florida mainland and opens north

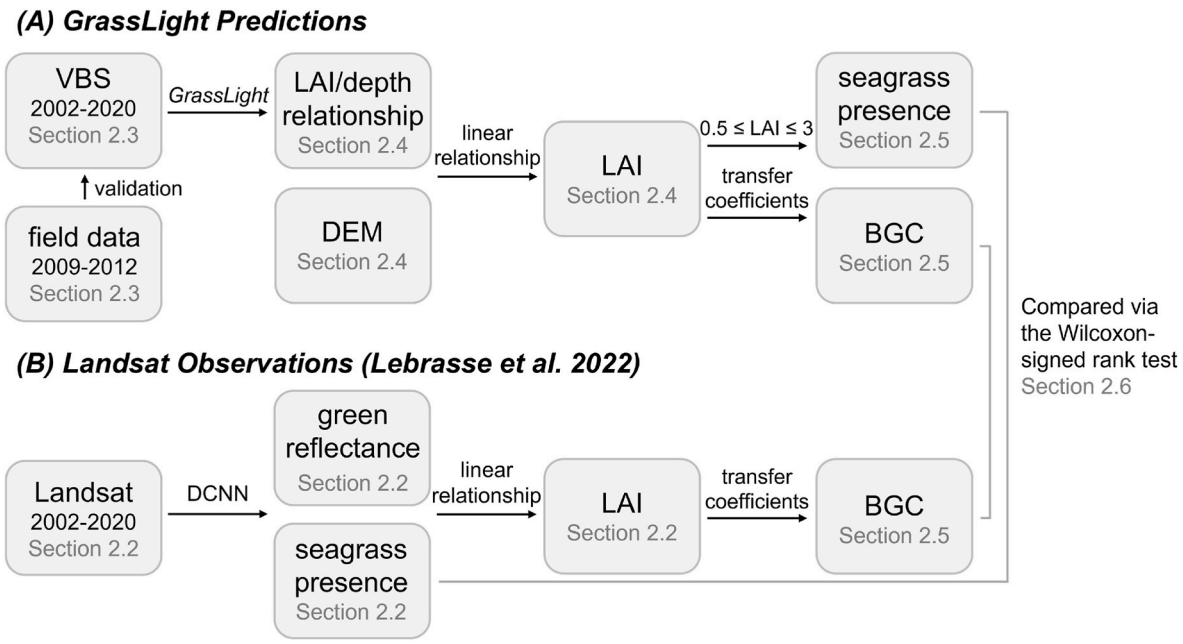

Fig. 1. Flowchart detailing the steps taken to compare *GrassLight* predictions of seagrass extent, LAI and BGC with corresponding observations derived from Landsat imagery (Lebrasse et al., 2022).

into the Gulf of Mexico (Fig. 2). Water temperatures range from winter lows around 8.5 °C to summer highs around 32 °C (Bologna, 1998), while salinities range from 22 to 35. St. Joseph Bay has a mean depth of 6.4 m and a maximum depth of approximately 10.7 m near the northern tip of the spit. The southern part of the bay provides a broad, shallow, sandy habitat that contains large seagrass meadows and patches of sand at an average depth of 0.9 m (Stewart and Gorsline, 1962; Valentine and Heck, 1993; Hill et al., 2014). Tides in St. Joseph Bay are diurnal with a mean amplitude of 0.5 m (Stewart and Gorsline, 1962; Valentine and Heck, 1993). Waves traveling northward through the Gulf of Mexico are refracted clockwise so that they arrive nearly parallel to the beach (Stewart and Gorsline, 1962). In general, the currents in St. Joseph Bay sweep around the St. Joseph Peninsula, producing a cyclonic circulation pattern in the bay (DEP, 2008). Current movement occurs on the surface throughout a major portion of the Bay, with no appreciable current except for the daily tide in most of the extensive shallow reaches of the southern end of the Bay (Stewart and Gorsline, 1962). Among the four seagrass species present in the coastal waters of West Florida, three species are present in St. Joseph Bay: *Thalassia testudinum* (turtlegrass), which is the dominant species, followed by *Halodule wrightii* (shoal grass) and *Syringodium filiforme* (manatee grass) (Savastano et al., 1984). *Halophila decipiens* (paddle grass) has not been observed in St. Joseph Bay (Zimmerman and Hill, pers. obs.).

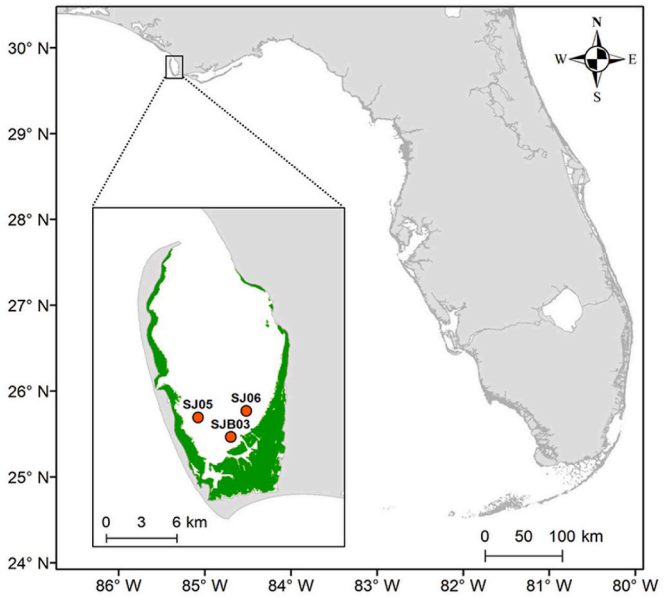

Fig. 2. Map of the state of Florida shoreline, with St. Joseph Bay shown in the inset. Orange points represent the location of Station SJB03 from the Virtual Buoy System (VBS) used as a source of water quality data for the *GrassLight* model and the locations of stations SJ05 and SJ06 from a 2009–2012 field survey (Schaeffer et al., 2015) that were used for *in situ* validation of the VBS water quality data. A 2010 map of seagrass extent, published by the Florida Fish and Wildlife Conservation Commission (FL FWC) is shown in green.

2.2. Satellite-based estimates of seagrass extent, biomass and carbon

Satellite-based estimates of seagrass extent, LAI, aboveground fresh biomass, and BGC were obtained using the approach described in Lebrasse et al. (2022). Briefly, 19 satellite images from Landsat 5 through 8 spanning 2002 through 2020 were classified into five classes (seagrass, sand, land, optically deep water and intertidal) on a pixel-by-pixel basis using a deep convolution neural network (DCNN; Islam et al., 2020). Classification agreement ranged from 90 to 96% compared to aerial imagery and high spatial resolution WorldView-2 imagery (Fig. 1). For satellite pixels classified as seagrass, LAI was estimated from the brightness of the green band as outlined in Dierssen et al. (2003) and Hill et al. (2014). Aboveground fresh biomass and BGC was estimated from LAI using the series of transfer coefficients described in section 2.5 below. Our analysis was confined to a subset of the results originally presented by Lebrasse et al. (2022) because water quality data for St. Joseph Bay required to run the *GrassLight* model were not available from the VBS before 2002.

2.3. Water quality parameters

Water quality parameters used as inputs to drive the *GrassLight* simulations in St. Joseph Bay were obtained from the University of South Florida VBS (https://optics.marine.usf.edu/; Hu et al., 2013),

which is based on their Virtual Antenna System that obtains data collected in near real-time (typically within 4–6 h of satellite overpass) from various multispectral satellite sensors. These satellite data are processed to generate regular water quality products for predefined regions of interest, including St. Joseph Bay (Hu et al., 2013). Out of the three VBS stations available for St. Joseph Bay, we used water quality estimates for station SJB03, which was located in the southern portion of the Bay closest to the densest seagrass meadows (Fig. 2). The water quality data products extracted from SJB03 include the absorption coefficient for CDOM at 443 nm ($a_{CDOM}(443)$, m^{-1}), sea surface temperature (SST, °C), turbidity (NTU), and Chl *a* (μgL^{-1}). These parameters were averaged for the six-month period between the spring (22–23 March) and the fall equinox (22–23 September) for each year from 2002 to 2020. Seagrasses are long-lived plants that accumulate significant carbon reserves to buffer against high frequency variations in light availability driven by water quality, hence, they integrate changes in water quality over time (Longstaff and Dennison, 1999). The *GrassLight* predictions represent steady-state densities based on clear sky light availability, water transparency derived from the VBS water quality data and metabolic carbon balance driven by photosynthesis and respiration (Fig. 1). Focusing our analysis on the six-month period preceding the fall equinox allowed consistent representation of average water quality conditions in St. Joseph Bay and for comparison with Landsat-derived seagrass density and biomass, which were also calculated for a date in the fall (Section 2.2 above).

Since water quality from the VBS station was estimated from the Moderate Resolution Imaging Spectroradiometer (MODIS) Aqua satellite (https://oceancolor.gsfc.nasa.gov), estimates of water quality from the VBS were validated against *in situ* measures of SST, Chl *a*, $a_{CDOM}(440)$, and turbidity obtained during a 2009–2012 field survey in St. Joseph Bay (Schaeffer et al., 2015). MODIS images coincident with *in situ* data were downloaded and the water quality parameters were extracted from them at the VBS location SJB03 for comparison with *in situ* data. Among the ten field stations sampled by Schaeffer et al. (2015), data from stations SJ05 and SJ06 were closest in proximity to SJB03 and were averaged for comparison. The MODIS SST product was used directly for this analysis, but Chl *a*, $a_{CDOM}(440)$, and turbidity were calculated from remote sensing reflectance (a measure of the water-leaving radiance normalized by the at-surface downwelling solar irradiance; R_{rs}) at 488, 547, 645 and 667 nm (Equations (1)–(3)).

$$a_{CDOM}(440)\left(m^{-1}\right) = B1 \times \left(0.7789 \times \left(\frac{R_{rs}\,(645)}{R_{rs}\,(488)}\right) - 0.0066\right) + B0 \quad (1)$$

$$\text{Chl}\ \ a\ \left(\mu g\ L^{-1}\right) = 8.8834 \times \left(\frac{R_{rs}(667)}{R_{rs}(547)}\right) \quad (2)$$

$$\text{Turbidity}\ \ (\text{NTU}) = 273.72 \times (R_{rs}(645) \times 0.866) \quad (3)$$

The MODIS-derived products were compared to the *in situ* measures using the mean absolute error (MAE) (Equation (4)) and the bias (Equation (5)), which have been found to be appropriate for evaluating ocean color algorithms (Seegers et al., 2018). The bias quantifies the mean of the absolute difference between the modeled and observed values, determining whether the algorithm tends to underestimate or overestimate the observed values. These statistical metrics do not amplify outliers and accurately reflect the error magnitude in ocean color algorithms (Seegers et al., 2018):

$$\frac{1}{n}\sum_{i=1}^{n}\left|y_i - x_i\right| \quad (4)$$

$$\frac{1}{n}\sum_{i=1}^{n}(y_i - x_i) \quad (5)$$

where y_i are modeled values, x_i are *in situ* observed values and n is sample size.

2.4. GrassLight simulations

The bio-optical model *GrassLight* Ver. 2.14 simulated the propagation and absorption of solar radiation through a vertically-defined seagrass canopy (Table 1) submerged in an optically homogeneous water column and the resulting metabolic balance between photosynthesis and respiration for the submerged plant canopy based on water temperature, pH, and shoot density (Zimmerman 2003a, 2006). It provides an accessible framework for understanding the relationship between water column optical properties, submerged plant canopies, and irradiance distribution in shallow waters. *GrassLight* successfully predicted the impact of water quality on eelgrass (*Zostera marina*) distribution in Dumas Bay Washington (Zimmerman 2003b) and Elkhorn Slough, California (Zimmerman, 2006), the distribution of turtlegrass in Florida Bay (McPherson et al., 2011), the combined impacts of temperature and ocean acidification on eelgrass (*Zostera marina*) abundance, distribution, and productivity in the Chesapeake Bay (Zimmerman et al., 2015) and the impacts of eelgrass metabolism on carbonate chemistry of Tomales Bay, California (Koweek et al., 2018). We used it here to predict the light-limited distribution and density of turtlegrass in St. Joseph Bay using the six-month averaged water quality parameters derived from the VBS following the procedure outlined in Zimmerman et al. (2015). LAI is defined as the ratio of leaf area (m^2) to the area of seabed (m^2). Although the bio-optical model can predict LAIs approaching 10 m^2 m^{-2} in extremely bright light environments, actual seagrass LAIs rarely exceed 3 m^2 m^{-2} (Beer and Waisel, 1982) largely due to physical space limitations required for roots and rhizomes in the sediments (Hemminga, 1998; Olesen et al., 2002). Consequently, we defined an LAI of 3 m^2 m^{-2} as the upper limit for seagrass density in these simulations.

Simulations to determine the maximum sustainable shoot density (the LAI at which the ratio of daily photosynthesis to respiration is equal to one, $P{:}R = 1$) for several sets of input conditions derived from the VBS (Table 2) were performed for depths ranging between 0.05 and 3 m, at intervals of 0.2 m, which encompassed the typical depth of seagrass colonization in St. Joseph Bay (Beck et al., 2018). The relationships between LAI and depth for each year derived from the *GrassLight* simulations were combined with a bathymetric digital elevation model (DEM; Hill et al., 2014) to propagate seagrass density across the submarine landscape, generating model grids for each scenario. The DEM, referenced to mean lower low water (MLLW), was downloaded from NOAA's bathymetric data viewer (https://www.ncei.noaa.gov/maps/bathymetry/) at 1-m resolution and resampled to a 30-m raster to match the spatial resolution of the Landsat-derived maps using an inverse distance weighting function implemented in ArcGIS (ESRI, 2016). The DEM has a vertical accuracy of 50 cm and a horizontal accuracy of 1 m (https://coast.noaa.gov/dataviewer/). The DEM was adjusted from MLLW to mean sea level (MSL) by adding 0.3 m to each grid cell, since the low to high tidal range averages 0.6 m in St. Joseph Bay.

Table 1
Parameter values assigned to each *GrassLight* simulation based on values in the literature. All runs were conducted for the fall equinox (12-h photoperiod).

Parameter	Value
Canopy height (mm)	300
Shoot leaf area (m^2/shoot)	0.001
Shoot: root ratio	0.33
Canopy orientation from vertical (°)	10
Leaf epiphyte load (mg cm^{-2})	1.238
pH	8.2
Sediment type	silica
Leaf optical properties	*Thalassia*

Table 2
Six-month mean water quality in St. Joseph Bay from station SJB03 of the University of South Florida Virtual Buoy System for the period between the spring and fall equinox between 2002 and 2020. SST is sea surface temperature, Chl *a* is chlorophyll *a*, and $a_{CDOM}(440)$ is chromophoric dissolved organic matter absorption coefficient at 440 nm. These input conditions were used in the *GrassLight* simulations.

6-month period	SST (°C)	Chl *a* ($\mu g L^{-1}$)	$a_{CDOM}(440)$ (m^{-1})	Turbidity (NTU)
23-Mar to 23-Sept-2002	26.0	3.19	0.44	1.6
23-Mar to 23-Sept-2003	25.9	4.08	0.95	1.79
22-Mar to 22-Sept-2004	25.8	2.9	0.50	2.17
22-Mar to 22-Sept-2005	25.3	4.05	0.69	1.84
23-Mar to 23-Sept-2006	26.3	2.73	0.47	2.25
23-Mar to 23-Sept-2007	25.5	2.82	0.46	2.18
22-Mar to 22-Sept-2008	25.4	3.2	0.55	2.28
22-Mar to 22-Sept-2009	25.7	3.27	0.62	1.78
22-Mar to 22-Sept-2010	25.9	3.41	0.61	2.06
23-Mar to 23-Sept-2011	26.3	3.05	0.56	2.14
22-Mar to 22-Sept-2012	26.2	3.02	0.51	1.88
22-Mar to 22-Sept-2013	25.2	3.92	0.65	1.97
22-Mar to 22-Sept-2014	25.7	3.43	0.61	2.01
23-Mar to 23-Sept-2015	26.4	3.59	0.66	1.93
22-Mar to 22-Sept-2016	26.4	3.58	0.68	2.05
22-Mar to 22-Sept-2017	26.0	3.31	0.54	2.02
22-Mar to 22-Sept-2018	26.2	3.07	0.47	2.22
23-Mar to 23-Sept-2019	26.6	3.38	0.57	1.88
22-Mar to 22-Sept-2020	26.8	2.76	0.64	1.88

2.5. GrassLight-based estimates of seagrass extent, seagrass biomass, and carbon

Total seagrass extent was calculated from the *GrassLight*-derived maps of LAI, where each grid cell with a LAI between 0.5 and 3 $m^2\ m^{-2}$ was reclassified as seagrass present (value = 1) throughout the model grid. Seagrass extent (km^2) was computed for each map by summing the number of seagrass grid cells and multiplying by the area of each 30 m grid cell (900 m^2).

Estimates of seagrass biomass and carbon were quantified from the LAI maps using a series of transfer coefficients that successively converted LAI to (i) aboveground fresh biomass (van Tussenbroek, 1998):

$$\text{Aboveground fresh biomass (Gg)} = 500\ (\text{g m}^{-2}\ \text{leaf}) \times \text{LAI}\ (\text{m}^2\ \text{leaf m}^{-2}\ \text{seabed}) \times 10^9 \quad (6)$$

(ii) Aboveground dry biomass (Sfriso and Ghetti 1998):

$$\text{Aboveground dry biomass (Gg)} = \text{Aboveground fresh biomass} \times 0.2 \quad (7)$$

And (iii) total aboveground organic carbon (Hemminga and Duarte, 2000; Howard et al., 2014):

$$\text{Aboveground organic carbon content (Gg C)} = \text{Aboveground dry biomass} \times 0.34 \quad (8)$$

Previous studies indicate a 10–20% uncertainty associated with conversions from LAI to biomass (Dierssen et al., 2003; Hill et al., 2014). In large and robust species that have an extensive root and rhizome system like *T. testudinum* (Zieman and Zieman, 1989; Kaldy and Dunton, 2000), belowground biomass can account for up to 88% of the total seagrass biomass (Collier et al., 2021). With 90% of the carbon in seagrass ecosystems being seagrass biomass, we estimated BGC by applying an aboveground to belowground (AGC:BGC) ratio of 1:3 based on a study of a *T. testudinum*-dominated seagrass meadow in an estuary with similar sedimentary characteristics to St. Joseph Bay (Equation (9); Folger, 1972; Zieman, 1975, 1982, 1989):

$$\text{BGC (Gg C)} = \text{Aboveground organic carbon content} \times 3 \quad (9)$$

The BGC estimates were extrapolated from LAI using coefficients from the literature and did not include burial of allochthonous algal and terrestrial detritus (Mazarrasa et al., 2018). The fresh biomass and BGC derived from the *GrassLight* predictions were compared to Landsat-derived fresh biomass and BGC.

2.6. Comparing GrassLight-derived and satellite-derived seagrass parameters

The nonparametric Wilcoxon signed-rank test was used to assess if there was substantive difference between *GrassLight*- and satellite-based estimates of seagrass extent, LAI, fresh biomass, and BGC (Wilcoxon, 1945) via the *rstatix* package in R version 4.0.0 (Kassambara and Kassambara, 2020; R Core Team, 2017). Cohen's *r* was used to quantify the difference between the two datasets in terms of effect size (Cohen, 1992). Cohen's *r* was calculated by dividing the *z*-score by the square root of the sample size, where the *z*-score was the measure of how many standard deviations a raw score was below or above the population mean. The results were interpreted according to the scheme introduced by Cohen (1988) for correlation coefficients where $|r| \geq 0.5$ indicates a strong effect; $0.3 \leq |r| < 0.5$ indicates a moderate effect, and $0.1 \leq |r| < 0.3$ indicates a weak effect.

2.7. Future climate scenario predictions

The impacts of climate warming and ocean acidification on seagrass extent and productivity in St. Joseph Bay were evaluated using *GrassLight* parameterized as in Table 1 but using the temperature and pH values for 2100 as forecasted by IPCC (2014). Temperature and pH anomalies were based on four RCPs (IPCC, 2014), which defined an estimate of radiative forcing based on a specific GHG emissions trajectory (Table 3).

In addition, the effects of declining water quality that might result from coastal development on seagrass extent and density were explored by increasing Chl *a*, $a_{CDOM}(440)$, and turbidity above the six-month

Table 3
Summary of the characteristics of each representative concentration pathway (RCP) generated by the IPCC (2014). The number that follows each RCP represents an estimated global sea surface temperature (SST) and pH anomaly for 2100, based on a specific greenhouse gas (GHG) emissions trajectory (in parts per million, ppm). Temperature and pH anomalies are given as the mean reported in IPCC (2014).

Pathway	Characteristics	SST anomaly (°C)	pH anomaly
RCP 2.6	very low GHG accumulation (490 ppm)	+1.0	−0.07
RCP 4.5	GHG concentrations stabilized at 650 ppm	+1.8	−0.15
RCP 6.0	GHG concentrations stabilized at 850 ppm	+2.2	−0.21
RCP 8.5	very high GHG accumulation (1370 ppm)	+3.7	−0.31

mean for September 22, 2020 in 20% increments, until the value of each parameter had doubled (Table 4); a 20% reduction in all parameters was also explored. These values were compared with values in the heavily disturbed seagrass ecosystems of Tampa Bay and Florida Bay, which have been subject to major seagrass loss over the past few decades due to degraded water quality (Johansson, 2002; Chen et al., 2007; Glibert et al., 2009; McPherson et al., 2011; Cole et al., 2018). A linear regression between the diffuse attenuation coefficient, K_dPAR, modeled from *GrassLight* for each percentage increase in Chl *a*, $a_{CDOM}(440)$, and turbidity as well as their corresponding seagrass extent and total leaf area were computed. Lastly, we combined the temperature and pH changes forecast under each RCP with the combined 100% increases in Chl *a*, $a_{CDOM}(440)$, and turbidity (worst-case water quality scenario) to evaluate these interactive effects on seagrass extent, total leaf area and BGC.

3. Results

3.1. Validation of water quality between field survey and Virtual Buoy System

The VBS appears to have produced reliable estimates of water quality parameters for St. Joseph Bay. The association between paired observations of field SST and MODIS SST had a slope of 1.0 and produced a mean absolute error (MAE) of 0.29 °C and a bias of 0.18 °C (Fig. 3a). Field Chl *a* was strongly correlated with MODIS Chl *a*, with a slope value of 0.94, MAE = 0.29 μgL^{-1}, and bias = −0.25 μgL^{-1} (Fig. 3b). A slope of 1 resulted from the comparison of field and MODIS $a_{CDOM}(440)$ with MAE = 0.20 m^{-1} and bias = 0.20 m^{-1} (Fig. 3c). The match-up comparison between field and MODIS turbidity produced the lowest slope (0.62) with MAE = 0.44 NTU and bias = −0.32 NTU (Fig. 3d). These results provide confidence for using the VBS data (Table 2) to drive the *GrassLight* simulations presented here.

3.2. LAI-depth relationship derived from GrassLight simulations

Mean water quality conditions for the six-month period preceding the fall equinox (Table 2) were used to drive the simulations, producing a depth profile for each year (Fig. 4a). Overall, the linear relationship between LAI and depth showed a relatively constant slope over the period from 2002 to 2020, with the maximum depth limit (i.e., the depth at which LAI decreased to zero) varying between 1.8 and 2.2 m from year to year (Fig. 4b). *GrassLight* predicted the submarine light environment of St. Joseph Bay in 2002 would have supported seagrass down to a depth of 2.2 m, which was the deepest limit found from 2002 to 2020. In 2003, the predicted depth limit for seagrass survival shallowed by 18% to 1.8 m, the shallowest among all years, and then deepened to 1.9 m in 2004. Based on the water column optical properties in 2005 and 2020, *GrassLight* predicted seagrass LAI down to an average depth limit of 1.95 m.

Table 4
Summary of the chlorophyll *a* (Chl *a*) concentrations, chromophoric dissolved organic matter absorption coefficient at 440 nm ($a_{CDOM}(440)$) and turbidity values used as inputs to *GrassLight* to predict seagrass leaf area index (LAI) and seagrass extent under declining water quality. Initial value represents the measured concentration for September 22, 2020.

Percentage increase or decrease	Water quality variable		
	Chl *a* (μgL^{-1})	$a_{CDOM}(440)$ (m^{-1})	Turbidity (NTU)
−20%	2.21	0.51	1.5
Initial	2.76	0.64	1.88
+20%	3.31	0.77	2.25
+40%	3.86	0.90	2.63
+60%	4.42	1.03	3.0
+80%	4.97	1.15	3.38
+100%	5.52	1.28	3.75

3.3. Comparing GrassLight predictions with Landsat observations

The LAI vs. depth relationships generated by *GrassLight* simulations (Fig. 4a) were combined with the DEM to calculate the effect of variation in water quality on the extent of potential seagrass habitat in St. Joseph Bay over the 2002 to 2020 period. The mean area of potential light-limited seagrass extent over the 18-year period was 38 km^2, 57% more than the average seagrass extent of 23.0 km^2 realized from Landsat imagery (Fig. 5a). The predicted inter-annual range in light-limited seagrass extent (36.2 km^2–39.2 km^2) was also narrower than the range (7.9–27.4 km^2) observed from the satellite imagery (Cohen's r = 0.88, $p < 0.0001$; Fig. 5a). Seagrass was always present in the broad shallow areas between the intertidal and the deep edge in both Landsat and *GrassLight*. The overpredictions of seagrass extent by *GrassLight* occurred mainly in the intertidal region where desiccation usually prevents seagrass colonization and along the deep edge of seagrass distribution that may be exposed to greater wave energy than on the shallow flats (Fig. 6). Note that there are some narrow unvegetated areas along the eastern shore of St. Joseph Bay and near the city of Port St. Joe where the Landsat classifications consistently indicated seagrass presence but where *GrassLight* indicated seagrass absence. Landsat may have falsely classified these areas as seagrass as a result of high CDOM concentrations in these waters near the Gulf County Canal that connects St. Joseph Bay to the Intracoastal Waterway.

The underwater light environment in St. Joseph Bay was also predicted to support a total seagrass leaf area of 101.9 km^2 (range = 96.1–110.4 km^2), 65% more than the total leaf area of 36.4 km^2 (range = 24.2–45.5 km^2) estimated from Landsat (Fig. 5b; Cohen's r = 0.88, $p < 0.0001$). Moreover, *GrassLight* predicted a mean light-limited LAI of 2.7 m^2 m^{-2}, compared to a mean LAI of 1.9 m^2 m^{-2} estimated from Landsat. Consequently, the fresh biomass and BGC derived from *GrassLight* predictions of seagrass extent and density were greater than the distribution of values from Landsat (Table S1). *GrassLight* predicted fresh biomass and BGC was 64% more than Landsat-derived estimates of the same parameters (Cohen's r = 0.88, $p < 0.0001$).

3.4. Water quality scenarios: effects of Chl a, $a_{CDOM}(440)$, and turbidity on seagrass extent and density

With all other water quality parameters kept constant, a 20% increase in Chl *a* concentration from the mean value of 2.76 to 3.31 μgL^{-1} (Table 4) increased K_dPAR from 0.861 m^{-1} to 0.872 m^{-1} and shallowed the depth limit for seagrass survival by 2% (Fig. 7a). However, this had no effect on the predicted seagrass extent, LAI distribution or total leaf area in the bay (Fig. 8a). A 40% increase in Chl *a* concentration to 3.86 μgL^{-1} resulted in a 3% increase in K_dPAR but only a 1% decline in seagrass extent, LAI and total leaf area (Fig. 8a). Doubling the Chl *a* concentration to 5.2 μgL^{-1} increased K_dPAR by 5%, causing the depth limit for seagrass survival to decrease by 6.3% (Fig. 7a), and seagrass extent and total leaf area to decline by 5% (Fig. 8a). Simulating improved water quality by decreasing Chl *a* concentration by 20% reduced K_dPAR by 1%, which had no noticeable change on seagrass extent or total leaf area (Fig. 8a,d). Subtracting the bias of 0.25 μgL^{-1} (Fig. 3) from the lowest and highest Chl *a* concentration showed that seagrass extent only varied by 0.5% while LAI varied by 1% (Fig. 7a).

With all other water quality parameters kept constant, a 20% increase in $a_{CDOM}(440)$ from 0.51 to 0.64 m^{-1} (Table 4) increased K_dPAR by 6%, thereby reducing seagrass extent and total leaf area by 2% (Figs. 7b and 8b). Increasing $a_{CDOM}(440)$ in 20% increments up to a doubling of a_{CDOM} caused depth limit for seagrass survival to shoal by up to 20% (Fig. 7b). Seagrass extent declined from 4 to 8% while LAI and total leaf area declined from 4 to 9% as $a_{CDOM}(440)$ increased (Fig. 8b). On the other hand, a 20% decrease in $a_{CDOM}(440)$ resulted in a 3% increase in seagrass extent and a 4% increase in total leaf area. Subtracting

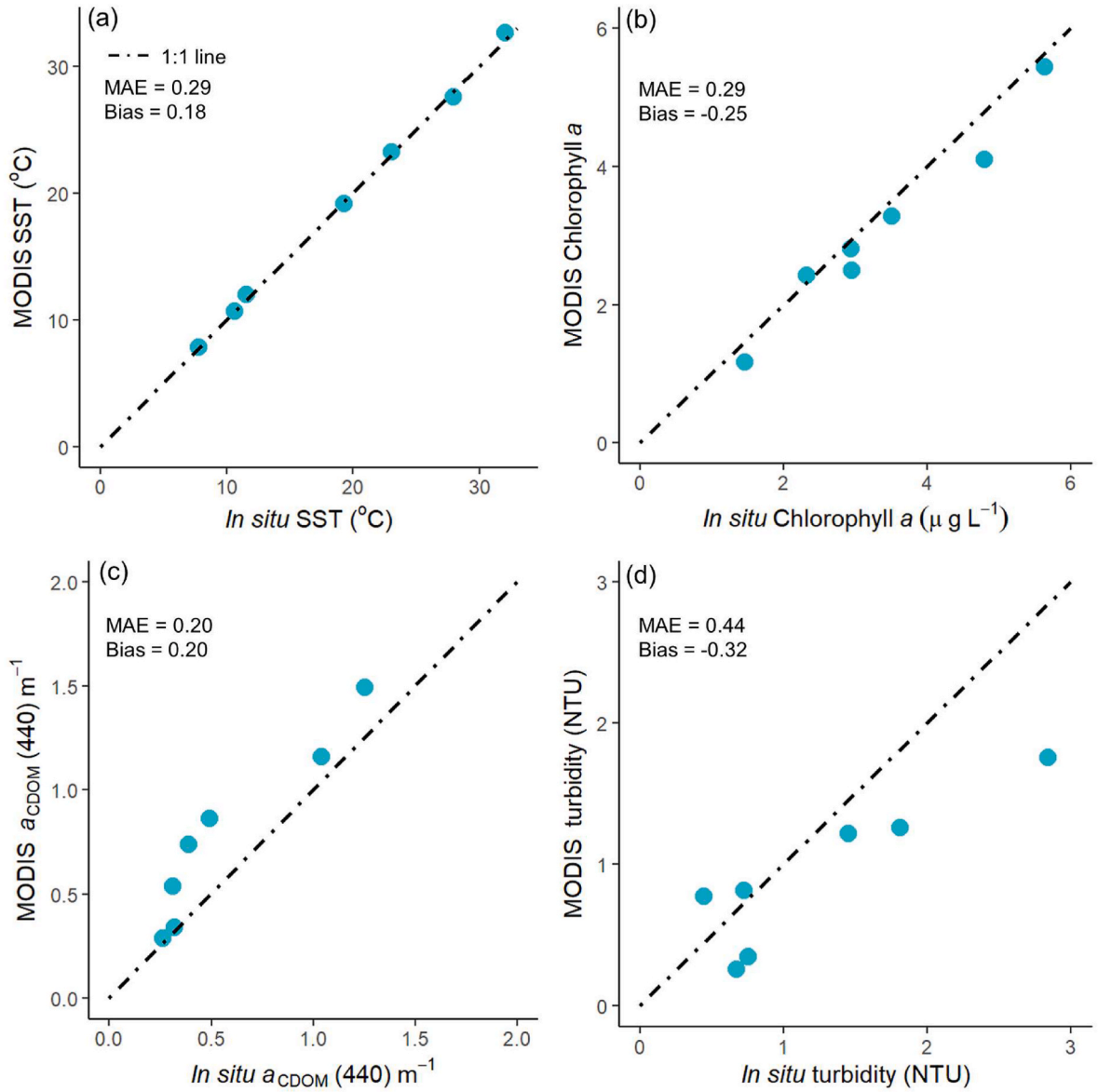

Fig. 3. Comparison between field data collected in St. Joseph Bay during 2009–2012 and data derived from the MODIS Aqua satellite for (a) sea surface temperature (SST), (b) Chlorophyll *a*, (c) chromophoric dissolved organic matter absorption coefficient at 440 nm ($a_{CDOM}(440)$) and (d) turbidity.

the bias of 0.20 m^{-1} (Fig. 3) from the lowest and highest $a_{CDOM}(440)$ values showed that seagrass extent only varied by 3% while LAI varied by 4% (Fig. 7b).

Increasing turbidity by 20% from the initial mean value of 1.88 to 2.25 NTU (Table 4) increased K_dPAR by 7% and reduced seagrass extent and total leaf area by 4% (Fig. 8c). Further increases in turbidity from the initial value up to a 100% increase led to an 18% decrease in seagrass extent and a 21% decrease in total leaf area (Fig. 8c). Consequently, the seagrass population in St. Joseph Bay appeared to be more sensitive to relative changes in total suspended matter than Chl *a* or $a_{CDOM}(440)$. Overall, results showed that among the three water quality metrics tested, a 100% increase in turbidity resulted in a 50% reduction in light and the largest decline in seagrass extent and total leaf area. However, seagrass extent and total leaf area expanded by 4% when turbidity was 20% below the initial mean value (Fig. 8c). Adding the bias of −0.32 NTU showed in Fig. 3 to the lowest and highest turbidity values showed that seagrass extent and total leaf area only varied by 3% and 4% respectively.

3.5. Climate scenarios

3.5.1. Scenario I: effects of temperature and pH

When considered in isolation, a 1 °C increase in SST (RCP 2.6) produced a 20% decrease in maximum colonization depth (Fig. 9a), a 2% decrease in total seagrass extent and 3% decrease in total leaf area and BGC (Fig. 10). A SST increase of 1.8 °C (RCP 4.5) caused seagrass extent and total leaf area to decline by 5% and 7%, respectively. Under RCP 6.0, SST increased by 2.2 °C, causing seagrass extent to decline by 6% and total leaf area to decline by 9% (Fig. 10a and b). Under the high GHG emissions scenario (RCP 8.5), seagrass extent declined by 8% and total leaf area declined by 13%.

When considered in isolation, climate change-induced acidification on the coastal waters of St. Joseph Bay increased seagrass extent and total leaf area under all RCP scenarios (Fig. 10). Seagrass extent increased by 3% while total leaf area and BGC increased by 4% under the low GHG emissions scenario (RCP 2.6). Under RCP 4.5, seagrass extent increased by 6% while total leaf area and BGC increased by 8% (Fig. 10). Seagrass extent increased by 8% while total leaf area and BGC increased by 11% with RCP 6.0. The high emissions scenario (RCP 8.5)

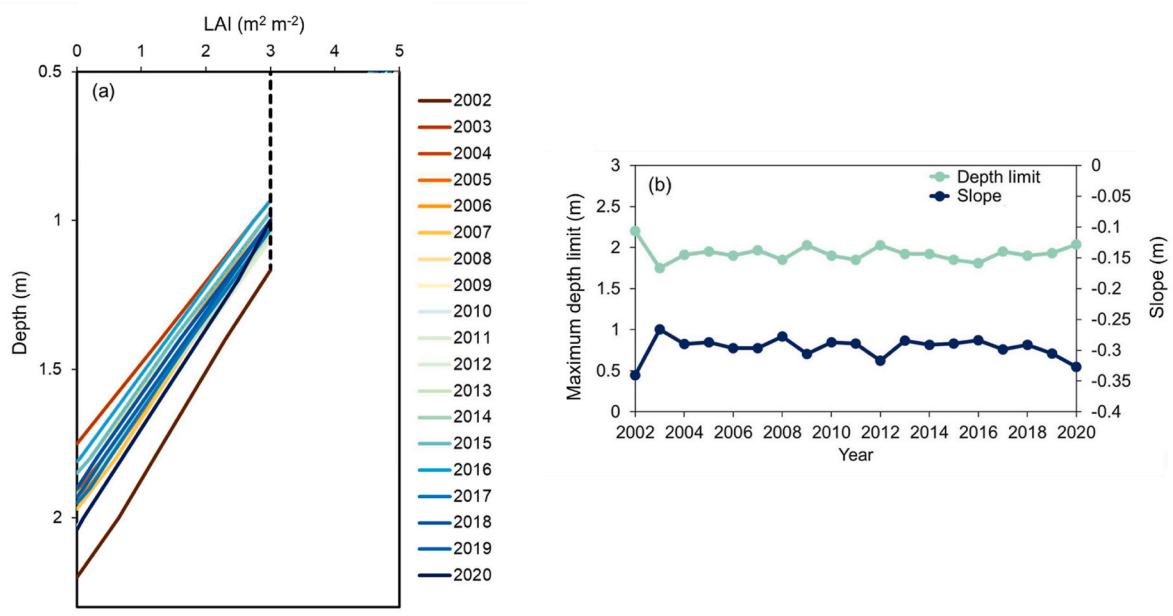

Fig. 4. (a) Depth profiles of maximum sustainable shoot density (defined as the leaf area index (LAI) value where ratio of daily Photosynthesis to Respiration = 1) for average water quality conditions for each simulation year from 2002 to 2020. An upper LAI threshold of 3 was used as the maximum seagrass density because the load of roots and rhizomes in the sediments generally does not allow seagrass plants to attain a higher LAI. (b) Time series of the maximum depth limit (intercept) and the slope derived from the depth profiles of maximum sustainable shoot density (LAI) between 2002 and 2020 as shown in Fig. 4a.

produced an 11% increase in seagrass extent and a 16% increase in total leaf area and BGC.

The combined effects of climate warming and ocean acidification resulted in an expansion of seagrass under the four RCP scenarios, indicating projected ocean acidification appears capable of offsetting the effects of projected thermal stress (Fig. 10). Only a 1% increase in seagrass extent, total leaf area, and BGC was predicted for 2100 under RCP 2.6 if pH and temperature were changed simultaneously. Under RCP scenarios 4.5 and 6.0, seagrass extent increased by 2–4% while total leaf area and BGC increased by 3–6%. The combined temperature increase and pH decrease forecasted under RCP 8.5 led to a 6% increase in total leaf area and a 9% increase in BGC.

3.5.2. Scenario II: simultaneous effects of temperature, pH, CDOM, Chl a, and turbidity

Combining the RCP 2.6 temperature and pH scenarios with 100% increases in Chl *a*, $a_{CDOM}(440)$, and turbidity decreased seagrass extent by 37% (Fig. 10a) and total leaf area by 45% (Fig. 10b). A 100% increase in Chl *a*, $a_{CDOM}(440)$ and turbidity combined with RCP 4.5 temperature and pH anomalies resulted in a 35% decrease in seagrass extent and 41% decrease in total leaf area and BGC (Fig. 10b and c). The temperature and pH anomalies associated with RCP 6.0 combined with a 100% increase in Chl *a*, $a_{CDOM}(440)$ and turbidity decreased seagrass extent by 33% (Fig. 10a) and total leaf area and BGC by 39% (Fig. 10b and c). When a 100% increase in Chl *a*, $a_{CDOM}(440)$, and turbidity was combined with the temperature and pH values projected under RCP 8.5, *GrassLight* predicted seagrass extent would decline by 31% (Fig. 10a) while total leaf area and BGC would decline by 35% (Fig. 10b and c). Mapping seagrass extent under each of these scenarios across the submarine landscape provided by the DEM showed a dramatic loss in seagrass extent in the southern portion of St. Joseph Bay when the worst-case water quality scenario was combined with each RCP scenario (Fig. 11). However, as simulations progressed from RCP 2.6 to RCP 8.5, seagrass extent, total leaf area, and BGC increased slightly even with the worst water quality conditions.

4. Discussion

Comparison of Landsat versus *GrassLight* model simulations showed that seagrasses in St. Joseph Bay may not be reaching their full light-limited potential (i.e., their maximum sustainable shoot density) and carbon storage capacity. Some possible explanations include exposure at low tide in shallow areas and wave action in deeper areas. Additionally, our *GrassLight* simulations showed that high temperature had a slight negative effect on seagrasses in St. Joseph Bay although the highest simulated temperature under RCP 8.5 was still within the optimum thermal tolerance for tropical seagrasses like *Thalassia*. The negative thermal stress was offset by a decrease in pH through climate-induced ocean acidification. Our simulations also showed that seagrasses were more sensitive to water quality than temperature and pH but a decrease in pH through ocean acidification may increase seagrass productivity to offset both the negative effects of thermal stress and declining water quality on the seagrasses growing in St. Joseph Bay.

4.1. Control of seagrass distribution and abundance in St. Joseph Bay

The *GrassLight* model indicated that the light availability and steady-state water quality in St. Joseph Bay were sufficient to support more extensive seagrass meadows than observed by Landsat. This was highlighted in the spatial difference maps between Landsat and *GrassLight,* which showed that *GrassLight* predicted seagrass colonization in the deep exposed areas where survival may be limited by wave energy (Infantes et al., 2009; Uhrin and Turner, 2018). This wave exposure effect has also been observed in the sand ripples and shoaling patterns visibly present in satellite imagery along the deep edges of the seagrass-inhabited areas (Hill et al., 2014; Coffer et al., 2020). Spatial differences in seagrass extent between Landsat and *GrassLight* also occurred in the intertidal region, where seagrasses in St. Joseph Bay may be subjected to the very high irradiance and desiccation during daytime low tides and extreme temperatures (both high and low) during low tide (Unsworth et al., 2012).

Similar to seagrass extent, *GrassLight* showed that the optical conditions and subsequent light regime in St. Joseph Bay were adequate to

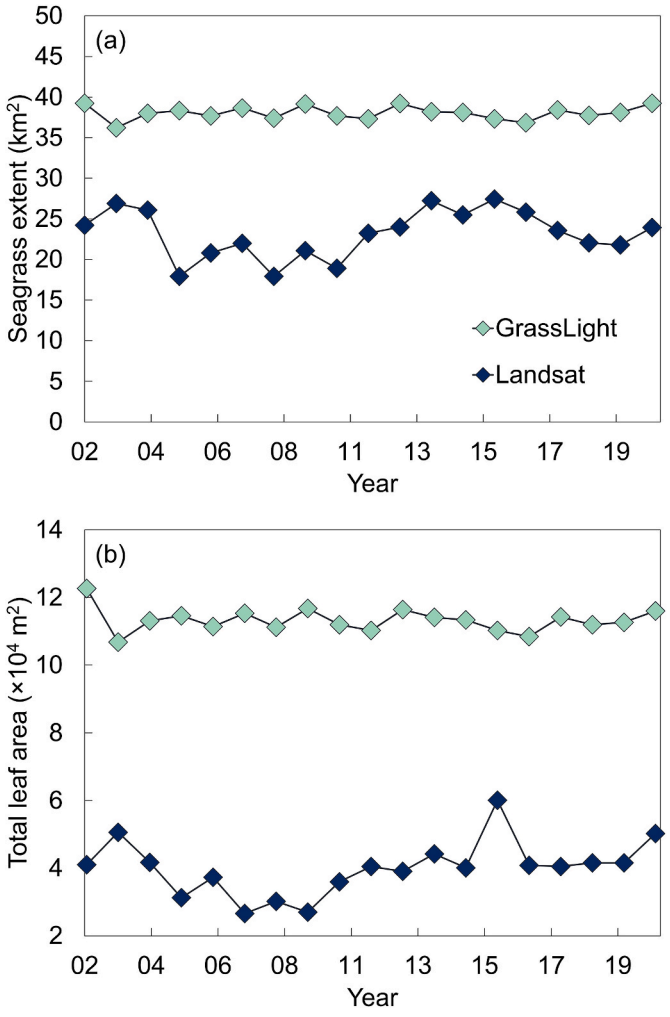

Fig. 5. Timeseries representing the distribution of (a) seagrass extent and (b) total leaf area derived annually from *GrassLight* between 2002 and 2020 based on water quality extracted from the Virtual Buoy System (VBS) for the six months preceding the fall equinox and derived from Landsat in Lebrasse et al. (2022).

support greater leaf area than what was estimated in Landsat imagery. In interpreting these results, it is important to emphasize here that these *GrassLight* predictions represent theoretical, light-limited seagrass densities for steady-state environmental conditions and consequently should be viewed as optimistic seagrass density limits. In addition, *GrassLight* does not consider other processes that may directly affect seagrass abundance such as physical disturbance from wave exposure (Infantes et al., 2009), grazing by increasingly abundant sea urchins and turtles (Heck and Valentine 1995; Rodriguez and Heck, 2020; 2021), or nutrient limitation (Fourqurean et al., 1992). Furthermore, seagrass densities and distribution mapped by Landsat represent snapshots of realized area that may not be in steady state with respect to the water quality parameters used to drive *GrassLight* predictions to light-limited densities (Zimmerman et al., 2015). Additionally, Landsat represents observations based on reflectance in the green band and it is possible that residual atmospheric contamination (Dierssen et al., 2003) may have caused the scenes to appear brighter than they really are, resulting in an underestimate of seagrass density (Coffer et al., 2020; Lebrasse et al., 2022). Still, the comparison between *GrassLight* and Landsat allowed us to identify areas within the bay where factors other than light may be important for seagrass growth.

4.2. Impact of water quality on seagrass distribution and abundance

Seagrasses along Florida's west coast, including St. Joseph Bay, are usually limited to the shallow nearshore and estuarine areas, where their distribution is largely determined by water clarity and light availability (Anastasiou, 2009), which is why improving water transparency has been the focus of monitoring and management efforts (Lefcheck et al., 2018; Sherwood et al., 2017; Greening et al., 2018; Tomasko et al., 2018). Although seagrass decline has been well documented throughout Florida, the seagrasses in St. Joseph Bay have been stable since at least 1993 (Yarbro and Carlson, 2016; Lebrasse et al., 2022). However, this long-term stability could be disrupted by the cumulative impacts of changing water quality and climatic conditions anticipated by the next century. Our model results in Fig. 7 showed that increasing light-attenuating parameters (Chl *a*, CDOM, and turbidity) reduced water clarity, which hindered light availability for seagrass photosynthetic activity and resulted in significant declines in seagrass extent and BGC in St. Joseph Bay. Chlorophyll, CDOM, and turbidity all contribute to the optical properties of coastal waters and characterize the underwater light climates to which seagrasses are highly sensitive. Although we showed that the water quality data retrieved from the VBS was slightly biased, incorporating this bias (which speaks to the uncertainty in the VBS retrieval) into the sensitivity analysis of each water quality metric (Chl *a,* CDOM, and turbidity) only changed the modeled seagrass extent and total leaf area by 0.5–4%. These results showed that the model results were relatively insensitive to the uncertainty associated with the VBS water quality parameters.

Using a 20–100% increase in CDOM, we showed how darkening of coastal waters threatens the survival of seagrasses in St. Joseph Bay. Coastal darkening has been reported to negatively impact phytoplankton growth due to reduced light availability, with consequences potentially propagating to the next trophic level (Mustaffa et al., 2020). Out of the three water quality conditions, turbidity had the highest impact on seagrass extent and total leaf area. There is evidence to suggest that sedimentation and turbidity will increase in many areas because of climate change (Basher et al., 2020). Our findings suggest that the anticipated increase in turbidity due to climate change would lead to conditions unfavorable for seagrass survival (Christian and Sheng, 2003; Tomasko et al., 2020).

The predicted impacts of water quality on St. Joseph Bay seagrass populations might appear to be less catastrophic than those reported for other locations such as Tampa Bay and Florida Bay, which have experienced increased input of nutrient and sediments associated with both coastal development and hurricanes in the past 40 years (Chen et al., 2007; Glibert et al., 2009; McPherson et al., 2011; Cole et al., 2018), causing major seagrass loss from degraded water quality (Johansson, 2002; Chen et al., 2007; Glibert et al., 2009). However, it is important to note that both the *highest* CDOM (1.28 m^{-1}) and Chl *a* (5.52 μgL^{-1}) values used for our St. Joseph Bay simulations were only slightly higher than the *lowest* CDOM (1.11–7.76 m^{-1}) and Chl *a* (4.6–25.1 μgL^{-1}) observed in Tampa Bay (Chen et al., 2007). Similarly, although increases in turbidity had the greatest impact on seagrass extent and density in our simulations, the highest simulated value (3.75 NTU) we used in St. Joseph Bay was half that commonly observed in Tampa Bay (4.6–7.2 NTU) and <33% of the value commonly observed in Florida Bay (12.21 NTU). Nonetheless, our simulations clearly illustrated that water quality deterioration will likely have a measurable, and perhaps greater, impact on seagrass resources in St. Joseph Bay than will climate change. For instance, inadequate water quality has been linked to widespread losses of seagrass coverage in two seagrass habitats on the Atlantic coast of Florida: The Indian River Lagoon (Lapointe et al., 2020) and Biscayne Bay (Santos et al., 2016). In St. Joseph Sound (located just west of Tampa Bay, approximately 300 km south of St. Joseph Bay), Tampa Bay, and Sarasota Bay, sustained efforts to reduce both point and non-point source nutrient loads have led to substantial improvements in both water quality and seagrass coverage (Tomasko and Keenan, 2019). The

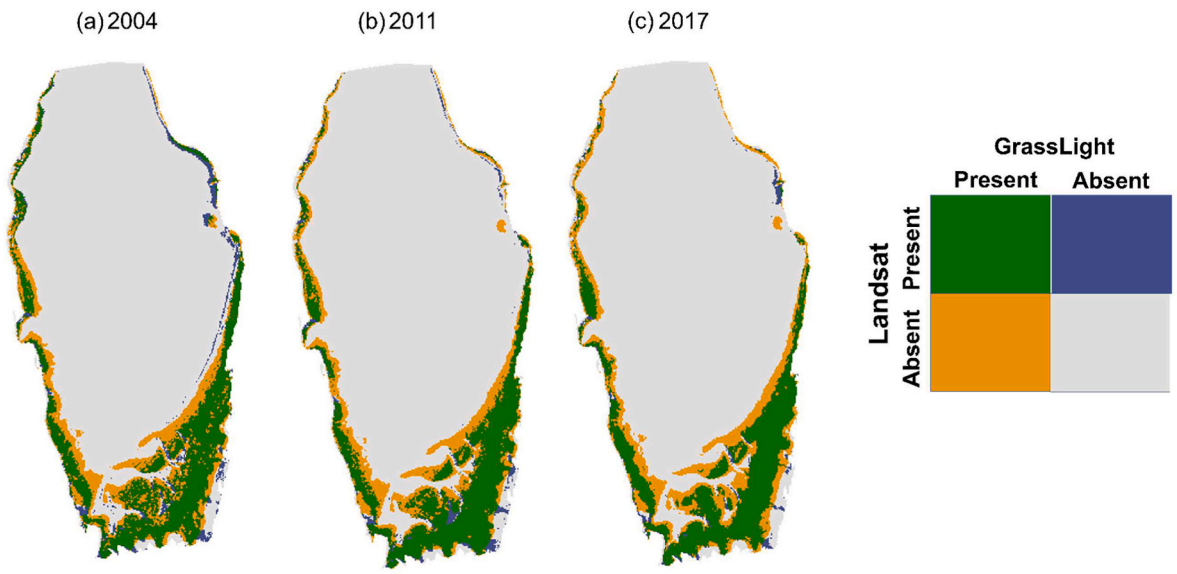

Fig. 6. Example of difference maps showing areas of agreement between Landsat-derived and *GrassLight*-derived seagrass extent for the year (a) 2004, (b) 2011, and (c) 2017.

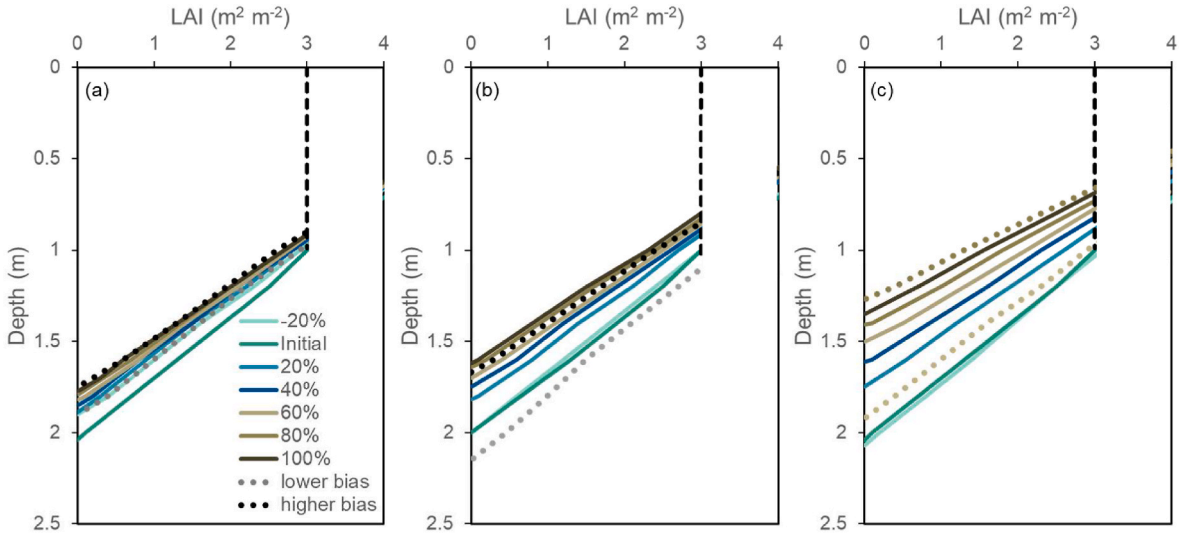

Fig. 7. Depth profiles of maximum sustainable shoot density (defined as the leaf area index (LAI) value where ratio of daily Photosynthesis to Respiration = 1) for incremental changes in (a) chlorophyll *a* (Chl *a*), (b) chromophoric dissolved organic matter absorption coefficient at 440 nm ($a_{CDOM}(440)$) and (c) turbidity from the initial value of September 22, 2020. The lower and higher bias represent the LAI-depth relationship resulting from correcting each of the three parameters according to the bias resulting from Fig. 3.

conservation and management implications of the latter suggest that improved water quality could make seagrass meadows more resilient to anticipated climate change. Consequently, the maintenance of adequate water quality conditions will continue to be a critical factor in perpetuating the stability and resilience of seagrass populations in St. Joseph Bay, which has been designated an Outstanding Florida Waterbody (OFW) and a Gulf of Mexico Ecological Management Site (GEMS) by the U.S. Environmental Protection Agency (DEP, 2008) due to the important commercial and recreational fish, invertebrates, wildlife and natural resources that its seagrasses support.

4.3. Effects of climate change on the future of seagrass in St. Joseph Bay

Temperature is a key factor for seagrass health, growth, and metabolic rate, and thermal stress generally depends on the species tolerance and its optimum temperature for metabolic activities (Lee et al., 2007; Carlson et al., 2018). Our simulations of a projected temperature increase (with constant water quality) in the next century had little impact on the seagrass extent and BGC storage of the tropical seagrass *Thalassia* in St. Joseph Bay. St. Joseph Bay is located relatively far north for the distribution of *Thalassia*, which typically requires an optimum temperature of 27–32 °C for photosynthesis (Zieman and Wood, 1975; Lee et al., 2007; Carlson et al., 2018). Since the maximum simulated temperature of 30 °C under RCP 8.5 was still within the optimum temperature range for *Thalassia,* this would explain why the simulated warming from *GrassLight* showed minimal impact for *Thalassia* in St. Joseph Bay. However, a threshold of approximately 35 °C has been suggested as the thermal tolerance of tropical seagrasses like *Thalassia* (Zieman and Wood, 1975; Koch et al., 2013; Fredley et al., 2019). For instance, Carlson et al. (2018) found that elevated temperatures of up to 38 °C were the likely cause of *Thalassia* mortality in the shallow mudbanks of western Florida Bay but not throughout the whole Bay. An earlier study

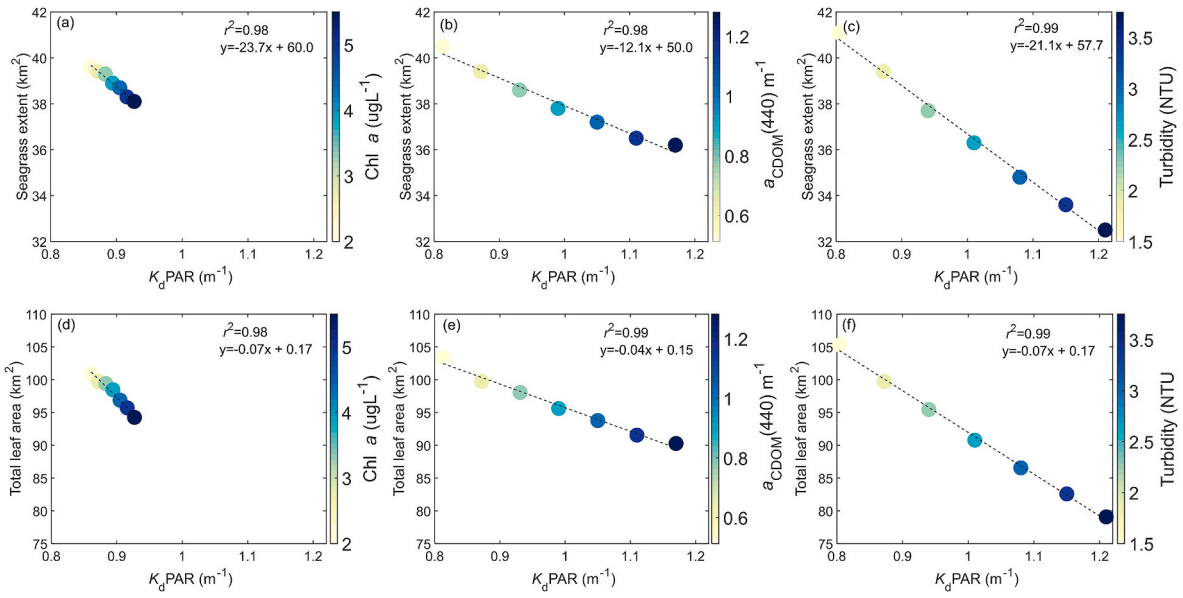

Fig. 8. Changes in (a–c) seagrass extent and (d–f) total leaf area with increasing K_dPAR caused by incremental changes (20–100%) in chlorophyll *a* (Chl *a*), chromophoric dissolved organic matter absorption coefficient at 440 nm ($a_{CDOM}(440)$) and total suspended matter. A 20% improvement in each water quality condition from the baseline conditions of September 22, 2020 was also simulated.

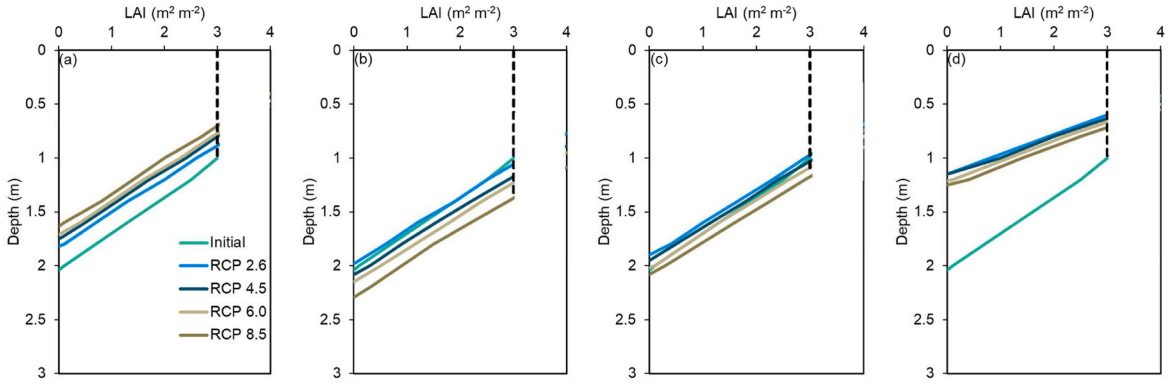

Fig. 9. Depth profiles of maximum sustainable shoot density (defined as the leaf area index (LAI) value where ratio of daily Photosynthesis to Respiration equals 1) for (a) temperature anomalies, (b) pH anomalies, (c) combined temperature and pH anomalies associated with each RCP scenario and (d) temperature and pH anomalies for each RCP combined with the worst-case water quality scenario as represented by a 100% increase in chlorophyll *a* (Chl *a*), chromophoric dissolved organic matter absorption coefficient at 440 nm ($a_{CDOM}(440)$), and turbidity. A threshold of 3 m^2 m^{-2} was used as the maximum seagrass density because the load of roots and rhizomes in the sediments generally does not allow seagrass plants to grow to a LAI greater than 3 m^2 m^{-2}.

reported mass mortality of *Thalassia* when temperatures reached 40 °C during extremely low summer tides in Puerto Rico (Glynn, 1968). Thus, it appears that even with the projected temperature increase under IPCC scenarios, the *Thalassia* seagrass beds of St. Joseph Bay will be resilient given their already high optimum temperatures; however, at temperatures at or beyond their thermal optima, they may be at risk of greater thermal stress (Collier et al. 2011, 2017; Pedersen et al., 2016). Such high temperatures could result from short-term marine heatwaves, which are becoming more frequent and extreme with climate change (Frölicher et al., 2018; Smale et al., 2019; Dzwonkowski et al., 2020), potentially pushing marine ecosystems like seagrasses to the limits of their tolerance (Arias-Ortiz et al., 2018).

While ocean acidification has been a major concern for other marine organisms, especially calcareous forms, our *GrassLight* model results showed that ocean acidification could benefit seagrass communities in St. Joseph Bay because seagrasses are photosynthetically CO_2-limited (reviewed in Zimmerman 2021). Due to the relatively low concentration of CO_2 in seawater and seagrasses' inefficient use of bicarbonate as an inorganic carbon source (Beer and Koch, 1996; Invers et al., 2001), the increased dissolution of CO_2 into surface waters, which is the more utilizable carbon for photosynthesis (Beer et al., 2002), increases the overall plant carbon balance of seagrasses as predicted by our *GrassLight* model simulations. Similar to our modeling study, laboratory, mesocosm, and field experiments have also shown increased photosynthetic activity in response to CO_2 (Zimmerman et al. 1997, 2017; Jiang et al., 2010; Fabricius et al., 2011; Russell et al., 2013). Although temperature and pH anomalies were simulated independently in this study, the reality is that they are both changing simultaneously when GHG emissions are increasing, through global warming and ocean acidification. Consequently, simulating simultaneous changes in temperature and pH under each RCP scenario showed that the negative effect of rising temperatures on seagrass extent, total leaf area, and BGC appeared to be compensated by a decreasing pH if both changes were happening concurrently by 2100. A similar response by seagrasses in the Chesapeake Bay was reported by Zimmerman et al. (2015), which found that ocean acidification would stimulate photosynthesis sufficiently to offset the negative effects of temperature increases on *Zostera marina*.

Coastal vegetated ecosystems like seagrasses are usually exposed to

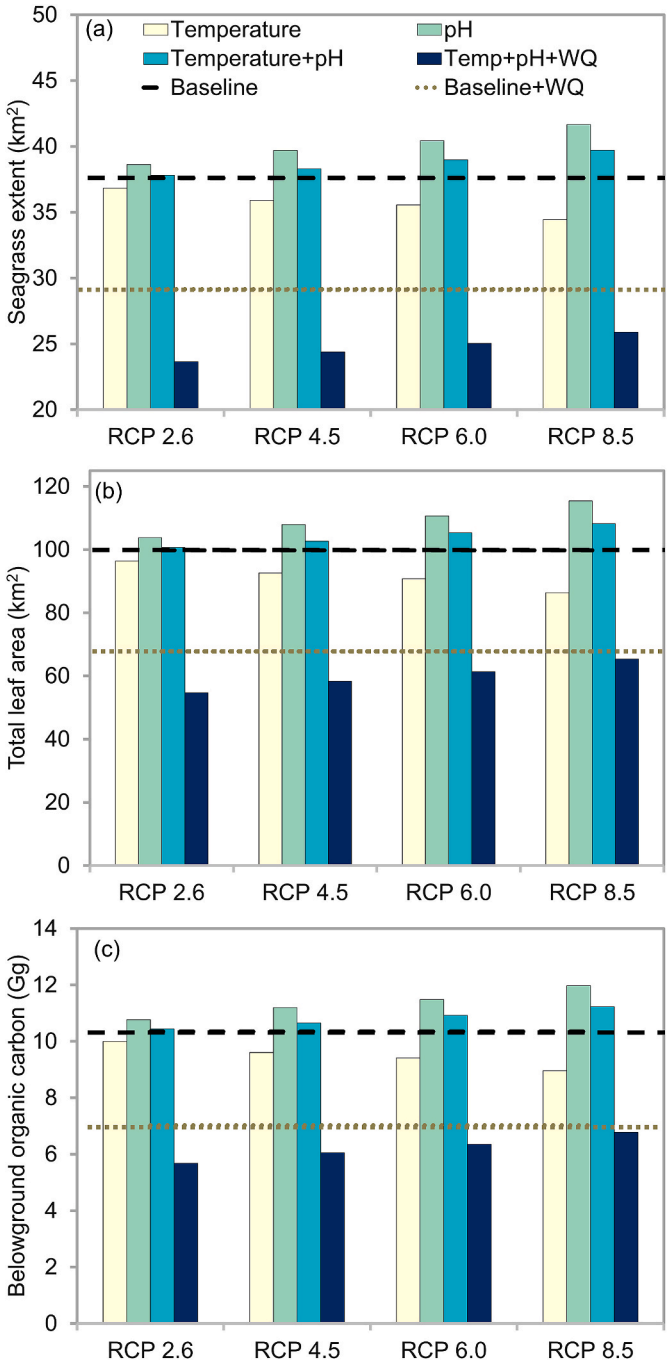

Fig. 10. Changes in (a) seagrass extent, (b) total leaf area, and (c) belowground organic carbon in St. Joseph Bay under temperature increases, pH decreases, and combined temperature and pH changes according to the four RCPs, as well as combined with declining water quality, represented by a 100% increase in chlorophyll *a* (Chl *a*), chromophoric dissolved organic matter absorption coefficient at 440 nm ($a_{CDOM}(440)$), and turbidity (worst-case water quality scenario). The black dashed line represents the baseline value for September 22, 2020 based on VBS water quality data and the brown dashed line represents the value when baseline temperature and pH for September 22, 2020 are combined with the worst-case water quality scenario.

more than one environmental or climate driver at a time, which makes it necessary to understand the response of seagrasses to multiple changes to effectively guide management and conservation efforts (Brodie et al., 2014). Our results suggest that the simultaneous exposure to higher temperature and lower pH would accelerate metabolic rates to cope with the negative impacts of declining water quality on seagrass growth. A similar antagonistic interaction was observed in *Cymodocea nodosa*, where acidification improved ammonium assimilation and buffered the enhanced respiration promoted by temperature (Egea et al., 2018). Overall, these results suggest that anthropogenic changes in water quality were a bigger stressor to seagrasses compared to temperature and pH, but also highlight that acidification can counteract combined anthropogenic and climate effects. Hence, predicting how anthropogenic and climate stressors interact to collectively impact on the extensive seagrass habitats of St. Joseph Bay should remain an area of focus for conservation efforts.

5. Conclusion

Our modeling approach using *GrassLight* represents an important advancement because it showed that when properly parameterized to accurately reproduce local environmental conditions, predictive models like *GrassLight* offer insights into the potential response of seagrass meadows to future climate change and water quality scenarios. With respect to St. Joseph Bay, *GrassLight* results showed that acidification has a large positive effect on the seagrasses while the warming temperatures associated with the IPCC climate scenarios has a smaller effect, mostly because the temperature range for the tropical seagrasses found in St. Joseph Bay exceed the climate warming projected by IPCC. Our results also showed that ocean acidification may increase seagrass productivity to offset both the negative effects of thermal stress and declining water quality on seagrass growing in St. Joseph Bay. Hence, the seagrass habitats of St. Joseph Bay could be resilient to expected climate changes if water quality is preserved. Healthy seagrasses in St. Joseph Bay will be necessary as other climate changes such as sea-level rise will require seagrasses to adapt to landward migration of the coastal landscape (Keyzer et al., 2020), more frequent and more intense tropical cyclones (Balaguru et al., 2016; Ting et al., 2019; Kossin et al., 2020), and potential changes in marine food webs (Du Pontavice et al., 2020).

The *GrassLight* modeling efforts presented in our study provide a predictive theoretical environment for evaluating the interactive effects of water quality, pH, and temperature on seagrass distribution, which is often difficult to observe *in situ* or remotely when all factors are changing simultaneously with independent trajectories (Zimmerman et al., 2015). Additionally, *in situ* experiments assessing the interactions between different stressors are rare due to experimental and budgetary constraints. Studies that use this type of multifactorial approach like *GrassLight* to model seagrass populations are needed to understand their resilience to future local and global environmental changes and to support management of their resources. However, the model did not attempt to capture the full suite of ecological, biogeochemical, and hydrodynamic processes occurring in seagrass meadows. As such, it should be viewed as a first effort to understand localized water quality and climate effects in a tropical seagrass meadow like St. Joseph Bay. Coupling a complex seagrass carbon model like *GrassLight* with an estuarine hydrodynamic model would provide more powerful biological and physical insights into the response of seagrasses to thermal stress, pH, and water quality changes. Unraveling local adaptation strategies of seagrasses in response to multiple stressors would be the next essential avenue to explore for seagrass conservation under a changing climate and increasing human pressures.

CRediT authorship contribution statement

Marie Cindy Lebrasse: Conceptualization, Methodology, Formal analysis, Software, Investigation, Data curation, Writing – original draft, preparation, Writing – review & editing. **Blake A. Schaeffer:** Conceptualization, Supervision, Writing – review & editing, Funding acquisition. **Richard C. Zimmerman:** Conceptualization, Supervision, Methodology, Writing – review & editing, Funding acquisition. **Victoria J. Hill:** Conceptualization, Methodology, Writing – review & editing. **Megan M. Coffer:** Conceptualization, Methodology, Writing – review &

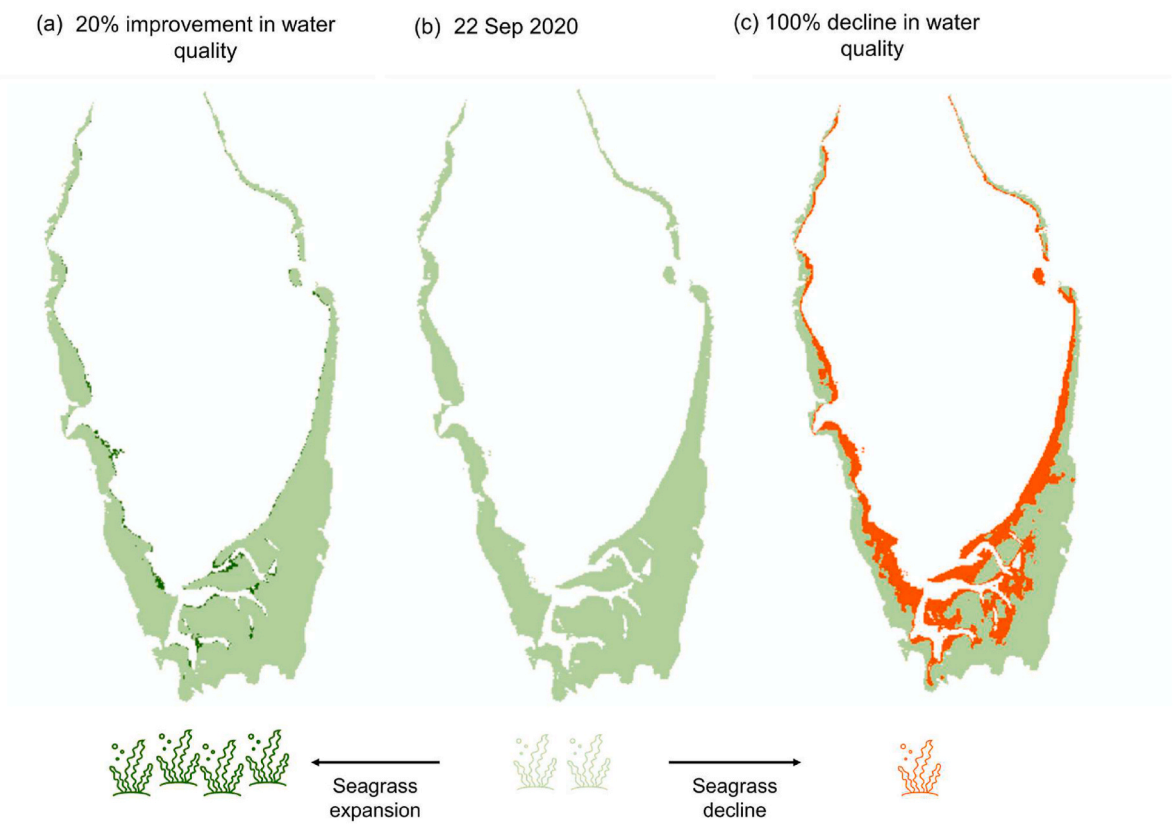

Fig. 11. Projected spatial changes in seagrass extent in St. Joseph Bay from baseline conditions on September 22, 2020. (a) Dark green represents areas where seagrass is projected to expand with a 20% improvement in water quality conditions. (b) Seagrass extent under baseline conditions on September 22, 2020. (c) Orange represents areas where seagrass is projected to be lost, under RCP 8.5 combined with the worst water quality scenario, as represented by a 100% increase chlorophyll *a* (Chl *a*), chromophoric dissolved organic matter absorption coefficient at 440 nm ($a_{CDOM}(440)$), and turbidity.

editing. **Peter J. Whitman:** Conceptualization, Methodology, Writing – review & editing. **Wilson B. Salls:** Conceptualization, Methodology, Writing – review & editing. **David D. Graybill:** Writing – review & editing. **Christopher L. Osburn:** Supervision, Writing – review & editing.

Declaration of competing interest

The authors declare that they have no known competing financial interests or personal relationships that could have appeared to influence the work reported in this paper.

Acknowledgement

The authors thank Dr. James Kaldy and Dr. James Hagy for their contribution in manuscript review. This work was supported by the NASA Ocean Biology and Biogeochemistry Program NRA #NNH16ZDA001N and augmented by the NASA Commercial Data Buy. Work was also supported by the National Science Foundation (OCE-2635403), U.S. EPA and Oak Ridge Institute for Science and Technology (ORISE). This article has been reviewed by the Center for Environmental Measurement and Modeling and approved for publication. Mention of trade names or commercial products does not constitute endorsement or recommendation for use by the U.S. Government. The views expressed in this article are those of the authors and do not necessarily reflect the views or policies of the U.S. EPA.

Appendix A. Supplementary data

Supplementary data to this article can be found online at https://doi.org/10.1016/j.marenvres.2022.105694.

References

Aksnes, D.L., Dupont, N., Staby, A., Fiksen, Ø., Kaartvedt, S., Aure, J., 2009. Coastal water darkening and implications for mesopelagic regime shifts in Norwegian fjords. Mar. Ecol. Prog. Ser. 387, 39–49.

Anastasiou, C.J., 2009. Characterization of the Underwater Light Environment and its Relevance to Seagrass Recovery and Sustainability in Tampa Bay. Florida. (Doctoral dissertation). https://digitalcommons.usf.edu/etd/1827.

Arias-Ortiz, A., Serrano, O., Masqué, P., Lavery, P.S., Mueller, U., Kendrick, G.A., Rozaimi, M., Esteban, A., Fourqurean, J.W., Marbà, N., 2018. A marine heatwave drives massive losses from the world's largest seagrass carbon stocks. Nat. Clim. Change 8 (4), 338–344.

Balaguru, K., Judi, D.R., Leung, L.R., 2016. Future hurricane storm surge risk for the US Gulf and Florida coasts based on projections of thermodynamic potential intensity. Climatic Change 138 (1), 99–110.

Barbier, E.B., Hacker, S.D., Kennedy, C., Koch, E.W., Stier, A.C., Silliman, B.R., 2011. The value of estuarine and coastal ecosystem services. Ecol. Monogr. 81 (2), 169–193.

Basher, L., Spiekermann, R., Dymond, J., Herzig, A., Hayman, E., Ausseil, A., 2020. Modelling the effect of land management interventions and climate change on sediment loads in the Manawatū–Whanganui region. N. Z. J. Mar. Freshw. Res. 54 (3), 490–511.

Beck, M.W., Odaya, M., 2001. Ecoregional planning in marine environments: identifying priority sites for conservation in the northern Gulf of Mexico. Aquat. Conserv. Mar. Freshw. Ecosyst. 11 (4), 235–242.

Beck, M.W., Hagy, J.D., Le, C., 2018. Quantifying seagrass light requirements using an algorithm to spatially resolve depth of colonization. Estuar. Coast 41 (2), 592–610.

Beer, S., Koch, E., 1996. Photosynthesis of marine macroalgae and seagrasses in globally changing CO_2 environments. Mar. Ecol. Prog. Ser. 141, 199–204.

Beer, S., Waisel, Y., 1982. Effects of light and pressure on photosynthesis in two seagrasses. Aquat. Bot. 13, 331–337.

Beer, S., Bjork, M., Hellblom, F., Axelsson, L., 2002. Inorganic carbon utilization in marine angiosperms (seagrasses). Funct. Plant Biol. 29 (3), 349–354.

Berger, A.C., Berg, P., McGlathery, K.J., Delgard, M.L., 2020. Long-term trends and resilience of seagrass metabolism: a decadal aquatic eddy covariance study. Limnol. Oceanogr. 65 (7), 1423–1438.

Blain, C.O, Hansen, S.C., Shears, N.T., 2021. Coastal darkening substantially limits the contribution of kelp to coastal carbon cycles. Global Change Biol. 27 (21), 5547–5563.

Bologna, P.A., 1998. Growth, production, and reproduction in bay scallops *Argopecten irradians concentricus* (say) from the northern Gulf of Mexico. J. Shellfish Res. 17 (4), 911–917.
Brand, L.E., Compton, A., 2007. Long-term increase in *Karenia brevis* abundance along the southwest Florida coast. Harmful Algae 6 (2), 232–252.
Brodie, J., Williamson, C.J., Smale, D.A., Kamenos, N.A., Mieszkowska, N., Santos, R., Cunliffe, M., Steinke, M., Yesson, C., Anderson, K.M., 2014. The future of the northeast Atlantic benthic flora in a high CO_2 world. Ecol. Evol. 4 (13), 2787–2798.
Campbell, J.E., Fourqurean, J.W., 2013. Effects of *in situ* CO_2 enrichment on the structural and chemical characteristics of the seagrass *Thalassia testudinum*. Mar. Biol. 160 (6), 1465–1475.
Capuzzo, E., Stephens, D., Silva, T., Barry, J., Forster, R.M., 2015. Decrease in water clarity of the southern and central North Sea during the 20th Century. Global Change Biol. 21 (6), 2206–2214.
Carlson, D.F., Yarbro, L.A., Scolaro, S., Poniatowski, M., McGee-Absten, V., Carlson Jr, P. R., 2018. Sea surface temperatures and seagrass mortality in Florida Bay: spatial and temporal patterns discerned from MODIS and AVHRR data. Remote Sens. Environ. 208, 171–188.
Chen, Z., Hu, C., Conmy, R.N., Muller-Karger, F., Swarzenski, P., 2007. Colored dissolved organic matter in Tampa Bay, Florida. Mar. Chem. 104 (1–2), 98–109.
Choice, Z.D., Frazer, T.K., Jacoby, C.A., 2014. Light requirements of seagrasses determined from historical records of light attenuation along the Gulf coast of peninsular Florida. Mar. Pollut. Bull. 81 (1), 94–102.
Christian, D., Sheng, Y.P., 2003. Relative influence of various water quality parameters on light attenuation in Indian River Lagoon. Estuar. Coast Shelf Sci. 57 (5–6), 961–971.
Coffer, M.M., Schaeffer, B.A., Zimmerman, R.C., Hill, V., Li, J., Islam, K.A., Whitman, P. J., 2020. Performance across WorldView-2 and RapidEye for reproducible seagrass mapping. Remote Sens. Environ. 250, 112036.
Cohen, J., 1988. Statistical power analysis for the behavioral sciences., 5. Lawrence Erlbaum Associates, Hillsdale, NJ.
Cohen, J., 1992. Statistical power analysis. Curr. Dir. Psychol. Sci. 1 (3), 98–101.
Cole, A.M., Durako, M.J., Hall, M.O., 2018. Multivariate analysis of water quality and benthic macrophyte communities in Florida Bay, USA reveals hurricane effects and susceptibility to seagrass die-off. Front. Plant Sci. 9, 630.
Collier, C.J., Uthicke, S., Waycott, M., 2011. Thermal tolerance of two seagrass species at contrasting light levels: implications for future distribution in the great barrier reef. Limnol. Oceanogr. 56 (6), 2200–2210.
Collier, C.J., Waycott, M., Ospina, A.G., 2012. Responses of four Indo-west Pacific seagrass species to shading. Mar. Pollut. Bull. 65 (4–9), 342–354.
Collier, C.J., Ow, Y.X., Langlois, L., Uthicke, S., Johansson, C.L., O'Brien, K.R., Hrebien, V., Adams, M.P., 2017. Optimum temperatures for net primary productivity of three tropical seagrass species. Front. Plant Sci. 8, 1446.
Collier, C.J., Langlois, L.M., McMahon, K.M., Udy, J., Rasheed, M., Lawrence, E., Carter, A.B., Fraser, M.W., McKenzie, L.J., 2021. What lies beneath: predicting seagrass below-ground biomass from above-ground biomass, environmental conditions and seagrass community composition. Ecol. Indicat. 121, 107156.
R Core Team, 2017. R: A Language and Environment for Statistical Computing. https://www.r-project.org/.
Davis, T.R., Harasti, D., Smith, S.D., Kelaher, B.P., 2016. Using modelling to predict impacts of sea level rise and increased turbidity on seagrass distributions in estuarine embayments. Estuar. Coast Shelf Sci. 181, 294–301.
de Los Santos, Carmen, B., Krause-Jensen, D., Alcoverro, T., Marbà, N., Duarte, C.M., Van Katwijk, M.M., Pérez, M., Romero, J., Sánchez-Lizaso, J.L., Roca, G., 2019. Recent trend reversal for declining European seagrass meadows. Nat. Commun. 10 (1), 1–8.
Dennison, W.C., Orth, R.J., Moore, K.A., Stevenson, J.C., Carter, V., Kollar, S., Bergstrom, P.W., Batiuk, R.A., 1993. Assessing water quality with submersed aquatic vegetation. Bioscience 43 (2), 86–94.
Dierssen, H.M., Zimmerman, R.C., Leathers, R.A., Downes, T.V., Davis, C.O., 2003. Ocean color remote sensing of seagrass and bathymetry in the Bahamas Banks by high-resolution airborne imagery. Limnol. Oceanogr. 48 (1part2), 444–455.
Du Pontavice, H., Gascuel, D., Reygondeau, G., Maureaud, A., Cheung, W.W., 2020. Climate change undermines the global functioning of marine food webs. Global Change Biol. 26 (3), 1306–1318.
Duarte, C.M., 1991. Seagrass depth limits. Aquat. Bot. 40 (4), 363–377.
Dzwonkowski, B., Coogan, J., Fournier, S., Lockridge, G., Park, K., Lee, T., 2020. Compounding impact of severe weather events fuels marine heatwave in the coastal ocean. Nat. Commun. 11 (1), 1–10.
Egea, L.G., Jiménez-Ramos, R., Vergara, J.J., Hernández, I., Brun, F.G., 2018. Interactive effect of temperature, acidification and ammonium enrichment on the seagrass Cymodocea nodosa. Mar. Pollut. Bull. 134, 14–26.
ESRI, 2016. ArcGIS Desktop: Release 10.8.1. *Environmental Systems Research Institute*, CA.
Fabricius, K.E., Langdon, C., Uthicke, S., Humphrey, C., Noonan, S., De'ath, G., Okazaki, R., Muehllehner, N., Glas, M.S., Lough, J.M., 2011. Losers and winners in coral reefs acclimatized to elevated carbon dioxide concentrations. Nat. Clim. Change 1 (3), 165–169.
FL DEP (Florida Department of Environmental Protection, 2008. St Joseph Bay Aquatic Preserve Management Plan. Tallahassee, FL. https://floridadep.gov/rcp/aquatic-preserve/locations/st-joseph-bay-aquatic-preserve.
Folger, D.W., 1972. Characteristics of Estuarine Sediments of the United States, vol. 724. US Government Printing Office, Washington, D.C, p. 94.
Fourqurean, J., Zieman, J., Powell, G., 1992. Phosphorus limitation of primary production in Florida Bay: evidence from C:N:P ratios of the dominant seagrass *Thalassia testudinum*. Limnol. Oceanogr. 37, 162–171.
Fraser, M.W., Kendrick, G.A., 2017. Belowground stressors and long-term seagrass declines in a historically degraded seagrass ecosystem after improved water quality. Sci. Rep. 7 (1), 1–11.
Fredley, J., Durako, M.J., Hall, M.O., 2019. Multivariate analyses link macrophyte and water quality indicators to seagrass die-off in Florida Bay. Ecol. Indicat. 101, 692–701.
Frölicher, T.L., Fischer, E.M., Gruber, N., 2018. Marine heatwaves under global warming. Nature 560 (7718), 360–364.
Glibert, P.M., Heil, C.A., Rudnick, D.T., Madden, C.J., Boyer, J.N., Kelly, S.P., 2009. Florida Bay: water quality status and trends, historic and emerging algal bloom problems. Contrib. Mar. Sci. 38, 5–17.
Glynn, P.W., 1968. Mass mortalities of echinoids and other reef flat organisms coincident with midday, low water exposures in Puerto Rico. Mar. Biol. 1 (3), 226–243.
Greening, H.S., Cross, L.M., Sherwood, E.T., 2011. A multiscale approach to seagrass recovery in Tampa Bay, Florida. Ecol. Restor. 29 (1–2), 82–93.
Greening, H., Janicki, A., Sherwood, E.T., 2018. Seagrass recovery in Tampa bay, Florida (USA). In: The Wetland Book: II: Distribution, Description, and Conservation. Springer, Dordrecht, pp. 495–506.
Griffiths, L.L., Connolly, R.M., Brown, C.J., 2020. Critical gaps in seagrass protection reveal the need to address multiple pressures and cumulative impacts. Ocean Coast Manag. 183, 104946.
Hall, M.O, Furman, B.T., Merello, M., Durako, M.J., 2016. Recurrence of Thalassia testudinum seagrass die-off in Florida Bay, USA: initial observations. Mar. Ecol. Prog. Ser. 560, 243–249.
Han, Q., Soissons, L.M., Bouma, T.J., van Katwijk, M.M., Liu, D., 2016. Combined nutrient and macroalgae loads lead to response in seagrass indicator properties. Mar. Pollut. Bull. 106 (1–2), 174–182.
Heck, K.L., Valentine, J.F., 1995. Sea urchin herbivory: evidence for long-lasting effects in subtropical seagrass meadows. J. Exp. Mar. Biol. Ecol. 189, 205–217.
Hemminga, M.A., 1998. The root/rhizome system of seagrasses: an asset and a burden. J. Sea Res. 39 (3–4), 183–196.
Hemminga, M.A., Duarte, C.M., 2000. Seagrass Ecology. Cambridge University Press.
Hill, V.J., Zimmerman, R.C., Bissett, W.P., Dierssen, H., Kohler, D.D., 2014. Evaluating light availability, seagrass biomass, and productivity using hyperspectral airborne remote sensing in Saint Joseph's Bay, Florida. Estuar. Coast 37 (6), 1467–1489.
Howard, J., Hoyt, S., Isensee, K., Telszewski, M., Pidgeon, E., 2014. Coastal blue carbon: methods for assessing carbon stocks and emissions factors in mangroves, tidal salt marshes, and seagrasses. Conservation International.
Hu, C., Barnes, B.B., Murch, B., Carlson, P.R., 2013. Satellite-based virtual buoy system to monitor coastal water quality. Opt. Eng. 53 (5), 051402.
Hughes, B.B., Lummis, S.C., Anderson, S.C., Kroeker, K.J., 2018. Unexpected resilience of a seagrass system exposed to global stressors. Global Change Biol. 24 (1), 224–234.
Infantes, E., Terrados, J., Orfila, A., Cañellas, B., Álvarez-Ellacuaria, A., 2009. Wave energy and the upper depth limit distribution of *Posidonia oceanica*. Bot. Mar. 52, 419–427.
Invers, O., Zimmerman, R.C., Alberte, R.S., Pérez, M., Romero, J., 2001. Inorganic carbon sources for seagrass photosynthesis: an experimental evaluation of bicarbonate use in species inhabiting temperate waters. J. Exp. Mar. Biol. Ecol. 265 (2), 203–217.
IPCC Core Writing Team, 2014. In: Pachauri, R.K., Meyer, L.A. (Eds.), Climate Change 2014: Synthesis Report. Contribution of Working Groups I, II and III to the Fifth Assessment Report of the Intergovernmental Panel on Climate Change. Geneva, Switzerland.
Islam, K.A., Hill, V., Schaeffer, B., Zimmerman, R., Li, J., 2020. Semi-supervised adversarial domain adaptation for seagrass detection using multispectral images in coastal areas. Data Sci. Eng. 5, 111–125.
Jiang, Z.J., Huang, X., Zhang, J., 2010. Effects of CO_2 enrichment on photosynthesis, growth, and biochemical composition of seagrass *Thalassia hemprichii* (Ehrenb.) Aschers. J. Integr. Plant Biol. 52 (10), 904–913.
Johansson, J., 2002. Historical overview of Tampa Bay water quality and seagrass issues and trends, p. 1-10. In: Greening, H.S. (Ed.), Proceedings, Seagrass Management, It's Not Just Nutrients! Symposium Held August 22-24, 2000. Tampa Bay Estuary Program, St. Petersburg, FL, p. 246.
Kaldy, J.E., Dunton, K.H., 2000. Above-and below-ground production, biomass and reproductive ecology of *Thalassia testudinum* (turtlegrass) in a subtropical coastal lagoon. Mar. Ecol. Prog. Ser. 193, 271–283.
Kassambara, A., Kassambara, M.A., 2020. Package 'ggpubr'. R Package Version 0.1 6.
Keyzer, L.M., Herman, P., Smits, B.P., Pietrzak, J.D., James, R.K., Candy, A.S., Riva, R., Bouma, T.J., van der Boog, C.G., Katsman, C.A., 2020. The potential of coastal ecosystems to mitigate the impact of sea-level rise in shallow tropical bays. Estuar. Coast Shelf Sci. 246, 107050.
Koch, M., Bowes, G., Ross, C., Zhang, X., 2013. Climate change and ocean acidification effects on seagrasses and marine macroalgae. Global Change Biol. 19 (1), 103–132.
Kossin, J.P., Knapp, K.R., Olander, T.L., Velden, C.S., 2020. Global increase in major tropical cyclone exceedance probability over the past four decades. Proc. Natl. Acad. Sci. USA 117 (22), 11975–11980.
Koweek, D.A., Zimmerman, R.C., Hewett, K.M., Gaylord, B., Giddings, S.N., Nickols, K.J., Ruesink, J.L., Stachowicz, J.J., Takeshita, Y., Caldeira, K., 2018. Expected limits on the ocean acidification buffering potential of a temperate seagrass meadow. Ecol. Appl. 28, 1694–1714.
Lapointe, B.E., Herren, L.W., Brewton, R.A., Alderman, P.K., 2020. Nutrient over-enrichment and light limitation of seagrass communities in the Indian River Lagoon, an urbanized subtropical estuary. Sci. Total Environ. 699, 134068.
Lebrasse, M.C., Schaeffer, B.A., Coffer, M.M., Whitman, P.J., Zimmerman, R.C., Hill, V.J., Islam, K.A., Li, J., Osburn, C.L., 2022. Temporal stability of seagrass extent, leaf area,

and carbon storage in St. Joseph Bay, Florida: a semi-automated remote sensing analysis. Estuar. Coast 1–20.
Lee, K., Park, S.R., Kim, Y.K., 2007. Effects of irradiance, temperature, and nutrients on growth dynamics of seagrasses: a review. J. Exp. Mar. Biol. Ecol. 350 (1–2), 144–175.
Lefcheck, J.S., Orth, R.J., Dennison, W.C., Wilcox, D.J., Murphy, R.R., Keisman, J., Gurbisz, C., Hannam, M., Landry, J.B., Moore, K.A., 2018. Long-term nutrient reductions lead to the unprecedented recovery of a temperate coastal region. Proc. Natl. Acad. Sci. USA 115 (14), 3658–3662.
Lefcheck, J.S., Hughes, B.B., Johnson, A.J., Pfirrmann, B.W., Rasher, D.B., Smyth, A.R., Williams, B.L., Beck, M.W., Orth, R.J., 2019. Are coastal habitats important nurseries? A meta-analysis. Conservation Letters 12 (4), e12645.
Longstaff, B.J., Dennison, W.C., 1999. Seagrass survival during pulsed turbidity events: the effects of light deprivation on the seagrasses Halodule pinifolia and Halophila ovalis. Aquat. Bot. 65 (1–4), 105–121.
Mazarrasa, I., Samper-Villarreal, J., Serrano, O., Lavery, P.S., Lovelock, C.E., Marbà, N., Duarte, C.M., Cortés, J., 2018. Habitat characteristics provide insights of carbon storage in seagrass meadows. Mar. Pollut. Bull. 134, 106–117.
McMahon, K., Lavery, P.S., Mulligan, M., 2011. Recovery from the impact of light reduction on the seagrass *Amphibolis griffithii*, insights for dredging management. Mar. Pollut. Bull. 62 (2), 270–283.
McPherson, M.L., Hill, V.J., Zimmerman, R.C., Dierssen, H.M., 2011. The optical properties of greater Florida Bay: implications for seagrass abundance. Estuar. Coast 34 (6), 1150–1160.
Moore, K.A., Shields, E.C., Parrish, D.B., Orth, R.J., 2012. Eelgrass survival in two contrasting systems: role of turbidity and summer water temperatures. Mar. Ecol. Prog. Ser. 448, 247–258.
Mustaffa, N.I.H., Kallajoki, L., Biederbick, J., Binder, F.I., Schlenker, A., Striebel, M., 2020. Coastal ocean darkening effects via terrigenous DOM addition on plankton: an indoor mesocosm experiment. Front. Mar. Sci. 841.
Nunes, J.P., Seixas, J., Keizer, J.J., Ferreira, A., 2009. Sensitivity of runoff and soil erosion to climate change in two Mediterranean watersheds. Part II: assessing impacts from changes in storm rainfall, soil moisture and vegetation cover. Hydrol. Process.: Int. J. 23 (8), 1212–1220.
Olesen, B., Enríquez, S., Duarte, C.M., Sand-Jensen, K., 2002. Depth-acclimation of photosynthesis, morphology and demography of *Posidonia oceanica* and *Cymodocea nodosa* in the Spanish Mediterranean sea. Mar. Ecol. Prog. Ser. 236, 89–97.
Orth, R.J., Carruthers, T.J., Dennison, W.C., Duarte, C.M., Fourqurean, J.W., Heck, K.L., Hughes, A.R., Kendrick, G.A., Kenworthy, W.J., Olyarnik, S., 2006. A global crisis for seagrass ecosystems. Bioscience 56 (12), 987–996.
Pacella, S.R., Brown, C.A., Waldbusser, G.G., Labiosa, R.G., Hales, B., 2018. Seagrass habitat metabolism increases short-term extremes and long-term offset of CO_2 under future ocean acidification. Proc. Natl. Acad. Sci. USA 115 (15), 3870–3875.
Paine, R.T., Tegner, M.J., Johnson, E.A., 1998. Compounded perturbations yield ecological surprises. Ecosystems 1 (6), 535–545.
Pedersen, O., Colmer, T.D., Borum, J., Zavala-Perez, A., Kendrick, G.A., 2016. Heat stress of two tropical seagrass species during low tides–impact on underwater net photosynthesis, dark respiration and diel *in situ* internal aeration. New Phytol. 210 (4), 1207–1218.
Petus, C., Collier, C., Devlin, M., Rasheed, M., McKenna, S., 2014. Using MODIS data for understanding changes in seagrass meadow health: a case study in the Great Barrier Reef (Australia). Mar. Environ. Res. 98, 68–85.
Prentice, C., Hessing-Lewis, M., Sanders-Smith, R., Salomon, A.K., 2019. Reduced water motion enhances organic carbon stocks in temperate eelgrass meadows. Limnol. Oceanogr. 64 (6), 2389–2404.
Rasmusson, L.M., Buapet, P., George, R., Gullström, M., Gunnarsson, P.C., Björk, M., 2020. Effects of temperature and hypoxia on respiration, photorespiration, and photosynthesis of seagrass leaves from contrasting temperature regimes. ICES (Int. Counc. Explor. Sea) J. Mar. Sci. 77 (6), 2056–2065.
Richardson, J.P., Lefcheck, J.S., Orth, R.J., 2018. Warming temperatures alter the relative abundance and distribution of two co-occurring foundational seagrasses in Chesapeake Bay, USA. Mar. Ecol. Prog. Ser. 599, 65–74.
Rodemann, J.R., James, W.R., Santos, R.O., Furman, B.T., Fratto, Z.W., Bautista, V., Hernandez, J.L., Viadero, N.M., Linenfelser, J.O., Lacy, L.A., Hall, M.O., Kelble, C.R., Kavanagh, C., Rehage, J.S., 2021. Impact of extreme disturbances on suspended sediment in western Florida Bay: implications for seagrass resilience. Front. Mar. Sci. 8 (633240), 2082–2094.
Rodriguez, A.R., Heck Jr., K.L., 2020. Green turtle herbivory and its effects on the warm, temperate seagrass meadows of St. Joseph Bay, Florida (USA). Mar. Ecol. Prog. Ser. 639, 37–51.
Rodriguez, A.R., Heck, K.L., 2021. Approaching a tipping point? Herbivore carrying capacity estimates in a rapidly changing, seagrass-dominated Florida Bay. Estuar. Coast 44 (2), 522–534.
Russell, B.D., Connell, S.D., Uthicke, S., Muehllehner, N., Fabricius, K.E., Hall-Spencer, J. M., 2013. Future seagrass beds: can increased productivity lead to increased carbon storage? Mar. Pollut. Bull. 73 (2), 463–469.
Santos, R.O., Lirman, D., Pittman, S.J., 2016. Long-term spatial dynamics in vegetated seascapes: fragmentation and habitat loss in a human-impacted subtropical lagoon. Mar. Ecol. 37 (1), 200–214.
Savastano, K.J., Faller, K.H., Iverson, R.L., 1984. Estimating vegetation coverage in St. Joseph Bay, Florida with an airborne multispectral scanner. Photogramm. Eng. Rem. Sens. 50.
Schaeffer, B.A., Conmy, R.N., Duffy, A.E., Aukamp, J., Yates, D.F., Craven, G., 2015. Northern Gulf of Mexico estuarine coloured dissolved organic matter derived from MODIS data. Int. J. Rem. Sens. 36 (8), 2219–2237.
Seegers, B.N., Stumpf, R.P., Schaeffer, B.A., Loftin, K.A., Werdell, P.J., 2018. Performance metrics for the assessment of satellite data products: an ocean color case study. Opt Express 26 (6), 7404–7422.
Sfriso, A., Ghetti, P.F., 1998. Seasonal variation in biomass, morphometric parameters and production of seagrasses in the Lagoon of Venice. Aquat. Bot. 61 (3), 207–223.
Sherwood, E.T., Greening, H.S., Johansson, J.R., Kaufman, K., Raulerson, G.E., 2017. Tampa Bay (Florida, USA) documenting seagrass recovery since the 1980's and reviewing the benefits. SE. Geogr. 57 (3), 294–319.
Short, F.T., Polidoro, B., Livingstone, S.R., Carpenter, K.E., Bandeira, S., Bujang, J.S., Calumpong, H.P., Carruthers, T.J., Coles, R.G., Dennison, W.C., 2011. Extinction risk assessment of the world's seagrass species. Biol. Conserv. 144 (7), 1961–1971.
Smale, D.A., Wernberg, T., Oliver, E.C., Thomsen, M., Harvey, B.P., Straub, S.C., Burrows, M.T., Alexander, L.V., Benthuysen, J.A., Donat, M.G., 2019. Marine heatwaves threaten global biodiversity and the provision of ecosystem services. Nat. Clim. Change 9 (4), 306–312.
Stewart, R.A., Gorsline, D.S., 1962. Recent sedimentary history of st. Joseph bay, Florida 1. Sedimentology 1 (4), 256–286.
Strydom, S., Murray, K., Wilson, S., Huntley, B., Rule, M., Heithaus, M., Bessey, C., Kendrick, G.A., Burkholder, D., Fraser, M.W., Zdunic, K., 2020. Too hot to handle: Unprecedented seagrass death driven by marine heatwave in a World Heritage Area. Global Change Biol. 26 (6), 3525–3538.
Ting, M., Kossin, J.P., Camargo, S.J., Li, C., 2019. Past and future hurricane intensity change along the U.S. East Coast. Sci. Rep. 9 (1), 1–8.
Tomasko, D.A., Keenan, E., 2019. Preliminary assessment of Sarasota bay water quality trends. https://sarasotabay.org/wp-content/uploads/2019-PreliminaryAssessment-of-Sarasota-Bay-Water-Quality-Trends-Memo.pdf, 21.
Tomasko, D.A., Corbett, C.A., Greening, H.S., Raulerson, G.E., 2005. Spatial and temporal variation in seagrass coverage in southwest Florida: assessing the relative effects of anthropogenic nutrient load reductions and rainfall in four contiguous estuaries. Mar. Pollut. Bull. 50 (8), 797–805.
Tomasko, D., Alderson, M., Burnes, R., Hecker, J., Leverone, J., Raulerson, G., Sherwood, E., 2018. Widespread recovery of seagrass coverage in southwest Florida (USA): temporal and spatial trends and management actions responsible for success. Mar. Pollut. Bull. 135, 1128–1137.
Tomasko, D., Alderson, M., Burnes, R., Hecker, J., Iadevaia, N., Leverone, J., Raulerson, G., Sherwood, E., 2020. The effects of Hurricane Irma on seagrass meadows in previously eutrophic estuaries in southwest Florida (USA). Mar. Pollut. Bull. 156, 111247.
Uhrin, A.V., Turner, M.G., 2018. Physical drivers of seagrass spatial configuration: the role of thresholds. Landsc. Ecol. 33 (12), 2253–2272.
Unsworth, R.K., Collier, C.J., Henderson, G.M., McKenzie, L.J., 2012. Tropical seagrass meadows modify seawater carbon chemistry: implications for coral reefs impacted by ocean acidification. Environ. Res. Lett. 7 (2), 024026.
Unsworth, R.K., Ambo-Rappe, R., Jones, B.L., La Nafie, Y.A., Irawan, A., Hernawan, U.E., Moore, A.M., Cullen-Unsworth, L.C., 2018. Indonesia's globally significant seagrass meadows are under widespread threat. Sci. Total Environ. 634, 279–286.
Unsworth, R.K., McKenzie, L.J., Collier, C.J., Cullen-Unsworth, L.C., Duarte, C.M., Eklöf, J.S., Jarvis, J.C., Jones, B.L., Nordlund, L.M., 2019. Global challenges for seagrass conservation. Ambio 48 (8), 801–815.
Valentine, J.F., Heck Jr., K.L., 1993. Mussels in seagrass meadows: their influence on macroinvertebrate abundance and secondary production in the northern Gulf of Mexico. Mar. Ecol.: Prog. Ser. 96, 63–74.
van der Heide, T., van Nes, E.H., Geerling, G.W., Smolders, A.J., Bouma, T.J., van Katwijk, M.M., 2007. Positive feedbacks in seagrass ecosystems: implications for success in conservation and restoration. Ecosystems 10 (8), 1311–1322.
van Tussenbroek, B.I., 1998. Above-and below-ground biomass and production by *Thalassia testudinum* in a tropical reef lagoon. Aquat. Bot. 61 (1), 69–82.
Waycott, M., Duarte, C.M., Carruthers, T.J., Orth, R.J., Dennison, W.C., Olyarnik, S., Calladine, A., Fourqurean, J.W., Heck, K.L., Hughes, A.R., 2009. Accelerating loss of seagrasses across the globe threatens coastal ecosystems. Proc. Natl. Acad. Sci. USA 106 (30), 12377–12381.
Webster, I.T., Harris, G.P., 2004. Anthropogenic impacts on the ecosystems of coastal lagoons: modelling fundamental biogeochemical processes and management implications. Mar. Freshw. Res. 55 (1), 67–78.
Wilcoxon, F., 1945. Some uses of statistics in plant pathology. Biometrics Bull. 1 (4), 41–45.
Wooldridge, S.A., 2017. Preventable fine sediment export from the Burdekin River catchment reduces coastal seagrass abundance and increases dugong mortality within the Townsville region of the Great Barrier Reef, Australia. Mar. Pollut. Bull. 114 (2), 671–678.
Yarbro, L.A., Carlson Jr., P.R., 2016. Seagrass Integrated Mapping and Monitoring Program: Mapping and Monitoring Report No. 2. Fish and Wildlife Research Institute. Technical Report TR-17 version 2. vi + 281 pp.
Zieman, J.C., 1975. Seasonal variation of turtlegrass, *Thalassia testudinum* König, with reference to temperature and salinity effects. Aquat. Bot. 1, 107–123.
Zieman, J.C., 1982. The Ecology of the Seagrasses of South Florida: A Community Profile. Department of the Interior, U.S. Fish and Wildlife Service, Office of Biological Services, Washington, D.C. FWS, p. 158. /CBS-82/25.
Zieman, J.C., Wood, E.F., 1975. Effects of Thermal Pollution on Tropical-type Estuaries, with Emphasis on Biscayne Bay. Elsevier Oceanography Series, Florida, pp. 75–98 (Elsevier).
Zieman, J., Fourqurean, J.W., Iverson, R.L., 1989. Distribution, abundance and productivity of seagrasses and macroalgae in Florida Bay. Bull. Mar. Sci. 44 (1), 292–311.

Zieman, T.C., Zieman, R.T., 1989. The ecology of the seagrass meadows of the west coast of Florida: a community profile, , 7th ed.85. US Department of the Interior, Fish and Wildlife Service, Research and Development.
Zimmerman, R.C., 2003a. A biooptical model of irradiance distribution and photosynthesis in seagrass canopies. Limnol. Oceanogr. 48 (1part2), 568–585.
Zimmerman, R.C., 2003b. Appendix M. Final Report. A bio-physical model evaluation of eelgrass distribution and habitat potential in Dumas Bay, WA. In: Berry, H.D., Sewell, A.T., Wyllie-Echeverria, S., Reeves, B.R., Mumford, T.F., Skalski, J.R., Zimmerman, R.C., Archer, J. (Eds.), Puget Sound Submerged Vegetation Monitoring Project: 2000 - 2003 Monitoring Report, 60 Pp Plus Appendices. Nearshore Habitat Program, Washington State Department of Resources, Olympia, WA.
Zimmerman, R., 2006. Chapter 13. Light and photosynthesis in seagrass meadows. In: Larkum, A., Orth, R., Duarte, C. (Eds.), Seagrasses: Biology, Ecology and Conservation. Springer, Dordrecht, pp. 303–321.
Zimmerman, R.C., 2021. Scaling up: predicting the impacts of climate change on seagrass ecosystems. Estuar. Coast 44 (2), 558–576.
Zimmerman, R.C., Kohrs, D.G., Steller, D.L., Alberte, R.S., 1997. Impacts of CO_2 enrichment on productivity and light requirements of eelgrass. Plant Physiol. 115 (2), 599–607.
Zimmerman, R.C., Hill, V.J., Gallegos, C.L., 2015. Predicting effects of ocean warming, acidification, and water quality on Chesapeake region eelgrass. Limnol. Oceanogr. 60 (5), 1781–1804.
Zimmerman, R.C., Hill, V.J., Jinuntuya, M., Celebi, B., Ruble, D., Smith, M., Cedeno, T., Swingle, W.M., 2017. Experimental impacts of climate warming and ocean carbonation on eelgrass Zostera marina. Mar. Ecol. Prog. Ser. 566, 1–15.